A Development of Non-intrusive Voltage Sensor for Energy Monitoring System

Sotara Ren

A Thesis Submitted in Partial Fulfillment of the Requirements for the Degree of Master of Engineering in Electrical Engineering

Prince of Songkla University

2018

Copyright of Prince of Songkla University

A Development of Non-intrusive Voltage Sensor for Energy Monitoring System

Sotara Ren

A Thesis Submitted in Partial Fulfillment of the Requirements for the Degree of Master of Engineering in Electrical Engineering

Prince of Songkla University

2018

Copyright of Prince of Songkla University

Thesis Title	A Development of Non-intrusive Voltage Sensor for Energy Monitoring System
Author	Mr. Sotara Ren
Major Program	Electrical Engineering

Major Advisor	**Examining Committee:**
………………………………	…..……………………………Chairperson
(Dr. Kittikhun Thongpull)	(Assoc. Prof. Kanadit Chetpattananondh)
	…..……………………………..Committee
	(Dr. Kittikhun Thongpull)
	…………………………………Committee
	(Assoc. Prof. Dr. Pornchai Phukpattaranont)
	…………………………………Committee
	(Prof. Dr. Prayoot Akkaraekthalin)

The Graduate School, Prince of Songkla University, has approved this thesis as partial fulfillment of the requirements for the Master of Engineering Degree in Electrical Engineering

…………………………………………..........

(Prof. Dr. Damrongsak Faroongsarng)

Dean of Graduate School

This is to certify that the work here submitted is the result of the candidate's own investigations. Due acknowledgement has been made of any assistance received.

..…..Signature
(Dr. Kittikhun Thongpull)
Major Advisor

..…..Signature
(Mr. Sotara Ren)
Candidate

I hereby certify that this work has not been accepted in substance for any degree, and is not being concurrently submitted in candidature for any degree.

…………………..………………..Signature

(Mr. Sotara Ren)

Candidate

Thesis Title	A Development of Non-intrusive Voltage Sensor for Energy Monitoring System
Author	Mr. Sotara REN
Major Program	Electrical Engineering
Academic Year	2017

ABSTRACT

Many technologies are nowadays moving towards to make easy ways to measure accurate power meter. There are two types of main waveforms (i.e. voltage and current waveform) are crucial to calculate power consumption in the smart meter system. The main aim of the smart meter makes users aware of the energy consumption on daily basis and to promote energy saving. As we knew that many proposed smart meters tried to obtain and create new methods, however, the majority acquire voltage waveform by cutting the cables. However, a number of research works proposed the concept of replacing the voltage transformer by the non-contact voltage sensor. The aim of this research is to study and develop a low-cost non-contact energy measurement system, which does not need any electrical contact with physical load or its conductor of power cables, obtain both voltage and current waveforms. We developed a contactless voltage sensor based on the parasitic capacitive-coupling technique. The proposed system achieved accurate power measurement, in fact, the error is approximately 2.5% compared with a standard wattmeter.

ACKNOWLEDGEMENTS

First, I would like to express the deepest appreciation to my grandparents, parents, sister, brother, and especially Oleak for their financial and mental/physical support since I was a child up to this moment.

A great appreciation is directly given to my advisor, Dr. Kittikhun Thongpull for encouragement, suggestion, guidance, understanding, and completing this subject even the social life in Thailand. I would also like to thank Prof. Dr. Prayoot Akkaraekthalin, Assoc. Prof. Dr. Pornchai Phukpattaranont, and Assoc. Prof. Kanadit Chetpattananondh for my comprehensive exam committee and giving advice that helped in addressing some of the shortcomings in the thesis. My special thanks go to Assist. Prof. Dr. Dujdow Buranapanichkit for giving me a chance to study here, and Assoc. Prof. Dr. Nattha Jindapetch, and Assoc. Prof. Dr. Krerkchai Thongnoo, and Asst. Prof. Dr. Kusumal Chalermyannont, and Dr. Warit Wichakool, and Dr. Rakkrit Duangsoithong for valuable advice, and teaching me.

I am heartily thankful to Miss. Salakjit Jeed Nilboworn, Mr. Kiattisa Sengchui, and Mr. Phichet Ketsamee for lab access and assessment. Many thanks go to all lecturers and friends either the nationals or internationals for their support, guidance, and love.

The financial supported from The Royal Scholarships under Her Royal Highness Princess Maha Chakri Sirindhorn Education Project to the Kingdom of Cambodia for Master Degree Program, Prince of Songkla University are gratefully acknowledged.

Finally, I hereby express my profound thank to all of them my well-done report. I wish them all with the fourfold blessing of Buddha: Longevity, Nobility, Peace, and Strength.

Sotara Ren

CONTENTS

Pages

LIST OF TABLES

Pages

LIST OF FIGURES

Pages

Pages

LIST OF ABBREVIATION

NILM	Non-intrusive load monitoring
ADC	Analog to digital converter
USB	Universal serial bus
IoT	Internet of thing
AC	Alternating current
JFET	Junction gate field-effect transistor
PIM	Plug-in the module
MCU	Microcontroller unit
GUI	Graphical user interface
PF	Power factor
rms	Root mean square
THD	Total harmonic distortion
SIND	Signal to noise and distortion

LIST OF SYMBOLS

L	Length of capacitive sensor
$\pm Q$	Column on the plate of the capacitor
N_P	Primary turns of the transformer
N_S	Secondary turns of the transformer
V_P	Primary voltage of the transformer
V_S	Secondary voltage of the transformer
a	Turns ratios of the transformer
R_1	Internal radius of the cable
R_2	External radius of the cable in Eq.3
C1	precision capacitor
V_{in}	Input voltage
R_2, R_3	Precision resistance in Eq.5
V_{outCC}	Output voltage (voltage follower)
$\cos\theta$	Power factor

CHAPTER 1
INTRODUCTION

1.1. Introduction

In the recent years, there have two directions such as smart grid and smart meter. These directions have distributed and managed the effort of the engineering communities in the electrical energy field. The usages of the electrical energy and the poor quality of the power transmission determine the waste of energy and low reliability of distribution systems. These reasons lead to visualize a new, to intelligent way to produce and to distribute the directions of the energy field. The smart meter is to promote more accurate of the resources and to make new awareness about the cost of the energy. Thus, among the first groups contributed to this concept, Non-Intrusive Load Monitoring (NILM) [1]. In addition, smart grids are expected to reveal the main characteristics, i.e. energy storage system, power system reliability, power quality, and renewable energy integration. The smart meters use a digital meter to record the real-time information. It can also provide a dynamic pricing and to remotely connect or disconnect the power load based on demand response [2]. In [3], smart meters measured voltage and current waveforms based on different working schemes needed to be digitized and processed by ADC or microcontroller.

According to [4], the authors measured voltage waveform designed with capacitive coupling. The voltage waveform was transferred via wireless transceiver with the IEEE 802.15.4 standard. Finally, the authors compared between their proposed non-intrusive methods and using direct access to the wire can achieve high accuracy with a maximum error lower than 1%. In [5], the authors discussed a technique to measure the 3-wire household power line without detached the insulation by using stray electric field energy harvesting. The authors also predicted that the non-intrusive voltage AC system could be applied to the smart grid system. According to [6], Gemini designed as a smart meter, which improved on accurately compute true power. Gemini marked the drawbacks of prior approached by decoupling and distributing the voltage and current measurement acquisitions to offer noninvasive technique.

The aim of this research is to develop the low-cost capacitive voltage sensor based on capacitive coupling sensor technique. Our design techniques measure the voltage and current waveform without intruding the cable. The voltage is measured using a noninvasive voltage sensor based on capacitive coupling element developed in this work, while a conventional current transformer is occupied for the current sensor.

1.2. Objectives and Scopes of Research

A new low-cost voltage sensor based on capacitive coupling, in a single line, is proposed. The voltage and current waveform will be monitored with the MCP3901 evaluation board 16bits MCU as illustrated in Figure 1.1. The MCP3901 evaluation board communicates with a computer via a Universal Serial Bus (USB) cable. The voltage and current waveform will be recorded with the board to analyze both data waveforms.

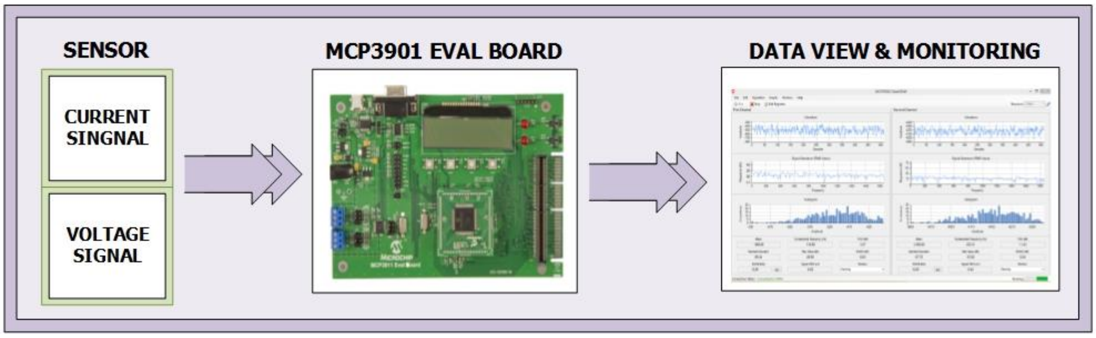

Figure 1.1: The block diagram

The design is capable of measuring voltage waveform without intruding the cable size. To complete this design, the parameters of research have to be determined the limited parameters of research as follows:

- Analyze the reliable energy usage from the voltage and current waveform
- Study the characteristics of the capacitive coupling
- Design an analog front-end

In order to achieve the goals, the different tasks have to be identified as following:

- The mathematical model of non-contactless capacitive coupling
- The behaviors of the parasitic capacitive sensor
- The behaviors of our proposed system
- The voltage and current waveform monitor with the MCP3901 evaluation board

CHAPTER 2
THEORY

2.1. Smart Meter

The smart meters use as a key element design for measuring power consumption data to record and analyze energy usage in the daily report. However, smart meters currently have limited settings to manage and measure power consumption i.e. the range of data logging maintenance according to the differences and changes of the appliances [3]. Many researchers consider that the power meters can also use only current drawn and ignore voltage levels. By the other way, the power meter can also not address the devices for implementation and customization. Thus, the authors can find the approaches of the smart meter, which the methodologies to find the necessary parameters are presented such as transformer and calibration factors. They have also expected that these approaches might also be applied for the customizable smart meter in the future. Other researchers also note that smart meters should have the quantity of their measurement, i.e. accurate data validation [7]. By the way, the key features of smart meters can be summarized as the time-based pricing, which easily provides the consumption data to the consumers and utilities. Looking at a last-meter proposed by [8], the authors designed an architecture and implementation of customer domain in the smart meters. This last- meter also applied an Internet of Things (IoT) platform to host in smart home applications. The authors also proposed 3 main parts of the platform such as the smart plug as sensor and actuator networks, IoT servers as a control server, and user interface as modifier and monitoring. The sensor and actuator communicated in the reliable IoT server by using gateway communication and displayed on a web-based graphical interface that made user-friendly as shown in Figure 2.1.

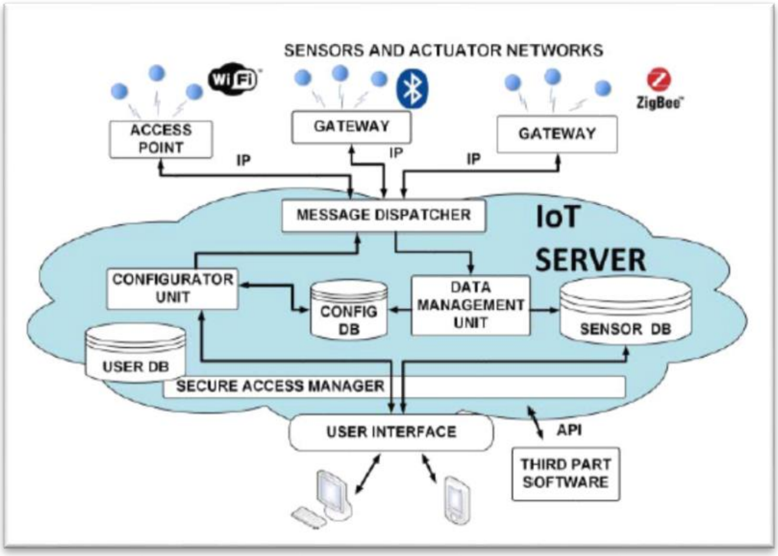

Figure 2.1: Communicated between IoT and Smart Meter [8]

In this platform, the authors applied the smart plug as the smart meter, which is implemented in home-prototype. The smart plug has monitored a load of information, which provided the active, reactive, and apparent power of phase. This smart plug has also measured power factor and sample waveforms with the root mean square value. The authors believed that the last-meter is the key to a widespread acceptance of smart grid applications and equipment to be developed at home. Furthermore, [9] mentioned that the smart meter was an electrical grid to deliver electrical in the controlled environment. The smart meter measures electronically the power consumption and possibly other parameters, in a certain time interval and transmits the measurement over a communication network to the utilities or the other responsibility for metering. This power information shared with the end-user devices to inform the customers about their power measurement and also related costs. Each type of smart meters is also different from the combination of some features or products such as the storage power consumption, communication types (i.e. one-way or multiple-ways), and connection with the providing supplier. The comparison between the traditional smart meters and the smart meters using 2-way communication with the smart meters and information to provide an automation and distribute advance energy delivery network is shown in Table 1.1 [10].

Table 1.1: Compared between smart meters and traditional meters [10]

Smart Meters	Traditional Meters
Digital	Electromechanical
Two-way communications	One-way communication
Distributed generation	Centralized generation
Sensor throughout	Few sensors
Self-monitoring	Manual monitoring
Self-healing	Manual restoration
Adaptive control	Failure and blackouts
Pervasive control	Limit control
Many customer choices	Few customer choices

2.2. Non-contact Voltage Measurement

2.2.1. Capacitor Principle

A capacitor is an electrical device for storing the electrical energy. In the similar components with resistor and inductor in an electric field, the capacitor is the very often-encountered component in the electrical circuit designs. By the way, the capacitor is used to smooth the current in rectified AC outputs, in the field of telecommunication, i.e. radio receivers. Next, the authors are also applied to the turning to requiring frequency such as the filters, time delay circuits, oscillator circuits, and checking body scanners, to name but a few practical application [11].

Every static electric field arises with the electric charges and the electrical field lines. Both electric charges and electrical field lines begin and end on the electric charges. Thus, these electric charges are provided with two plates, which is the description of the field each of the fields indicated between the negative and positive electric charges as namely capacitor (see Figure 2.2).

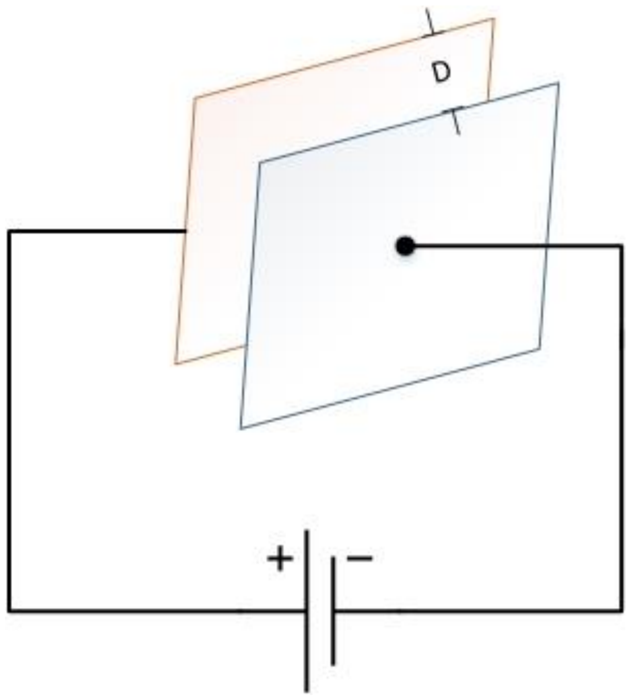

Figure 2.2: The two parallel conducting plate separate by air

The capacitor is also one of the electrical components that have one or more plates of the conductor. This conductor separated by an insulator and it is used to collect the electrical charge. The capacitor was charged as +Q coulombs on each plate and –Q coulombs on the different side of the other plate. Thus, the capacitance is the properties of these pairs of plates that determine how much correspond to a given voltage between these conductor plates. The capacitance can also be proportional to the change between an electrical charge (Q) and its electric potential (V) of a system. The capacitance value is given as follows:

$$C = \frac{Q}{V} \quad (1)$$

The unit of capacitance is measured as farad (F) which defined as the capacitance. It means that one coulomb charged with a voltage of one volt appear across the capacitance plates.

2.2.2. Capacitive Voltage Sensor

The capacitive voltage sensors are very often used to obtain the voltage waveform in a wire or piece of equipment. The capacitive voltage sensors also make with the non-contact of the direction and the conductor or the part of the electrical energy. The capacitance-voltage sensor has been the standard for high accuracy electrostatic potential measurements. By the way, the cost of material is are more expensive and their accuracy is also very dependent. The authors found the voltage changed about 5 percent over between the sensor and the surface of the capacitive distance of 3mm to 30mm [12]. There are many papers studied the traditional single capacitive measurement approach. However, this approach is not an accurate measurement and can easily be made a difference to the many environmental factors. However, the two-sensor head capacitive probe has been developed. Moreover, the authors also mention the accuracy of these capacitive voltage sensors in the AC voltage system as mentioned in Figure 2.3. With adding these sensor heads, the sensed voltage measurement is less sensitive to the medium of the sensing condition and the distance between the sensing surface and the sensor. The results are able to reduce the estimation error to around 5% [13].

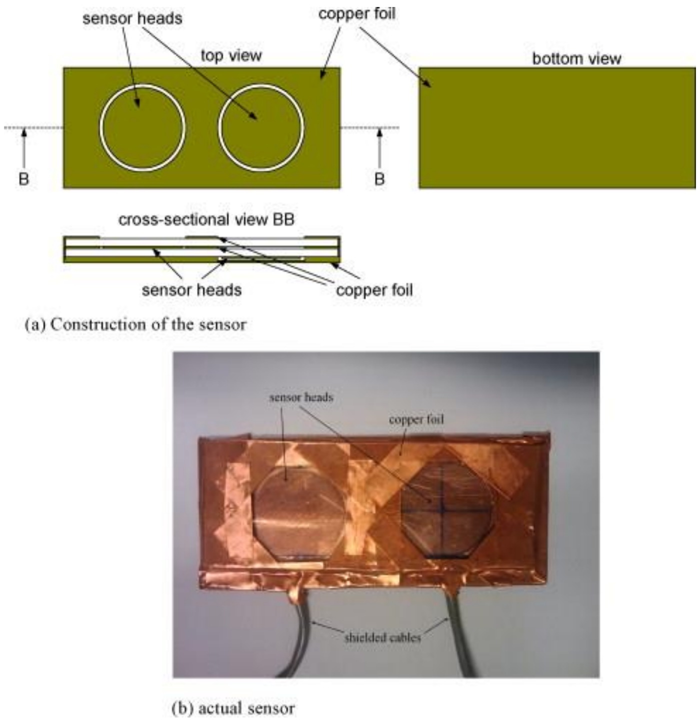

Figure 2.3: (a) Prototype of the sensor; (b) Real capacitive sensor [13]

It is a completely non-invasive and self-power meter which capable of sensing in a non-contact manner [14]. The extension of the ADC front-end permits the usage for the mono-phase electrical load intruding the cable by using the capacitive coupling. The software on board elaborated the current waveform and then computed some power quality features of the electric load, i.e. the power consumption as shown in Figure 2.4. The authors also obtained the cylindrical capacitor situated between the inner side of the copper plate of radius, R_2 and the surface of the conductive wire of the cable for radius R_1. The insulating of the cable, with permittivityε, separates these radii as mentioned.

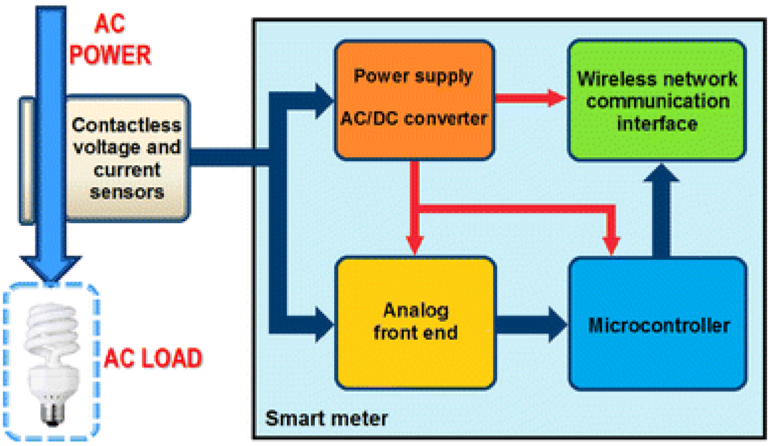

Figure 2.4: The block diagram of the single-phase meter [14]

The capacitive coupling on both sides of cables on the power lines was wrapped; after that, both capacitive couplings to the differential input system were attached to each other shown in Figure 2.5. By the way, the analog front-end of this system is illustrated in Figure 2.6.

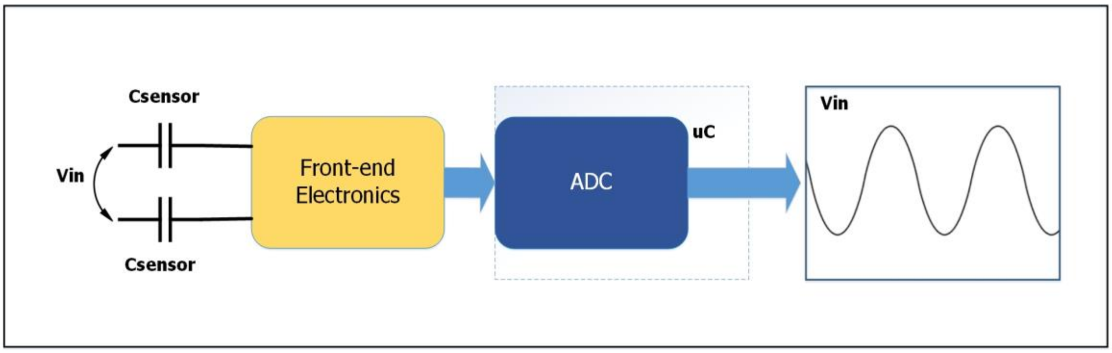

Figure 2.5: Diagram of the voltage measurement

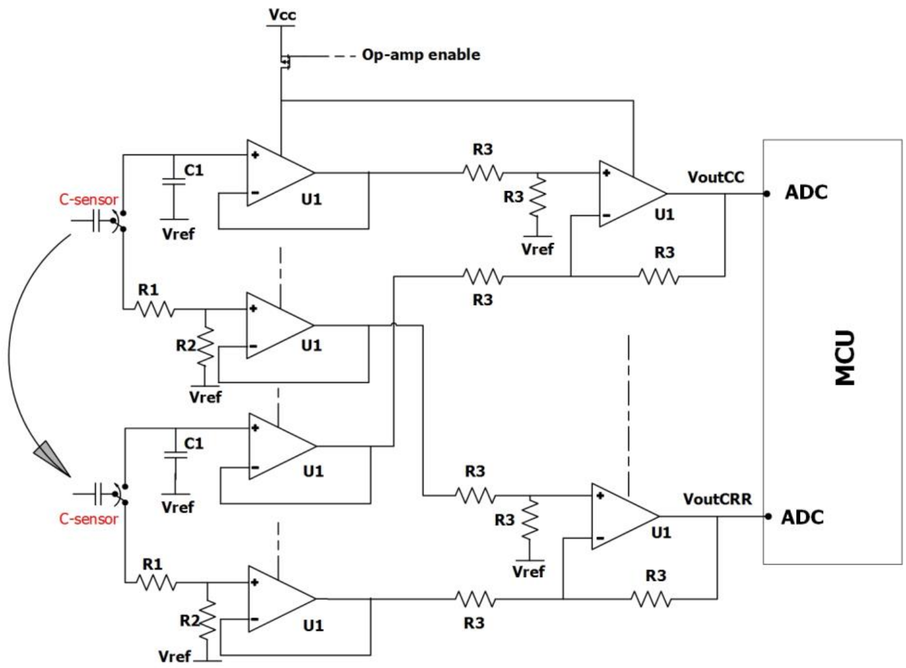

Figure 2.6: The design contactless voltage measurement system [14]

According to the literature [15]- [16]- [17], the researchers proposed the smart power consumption measured the power meter from voltage and the current sensor in three-phase as shown in Figure 2.7.

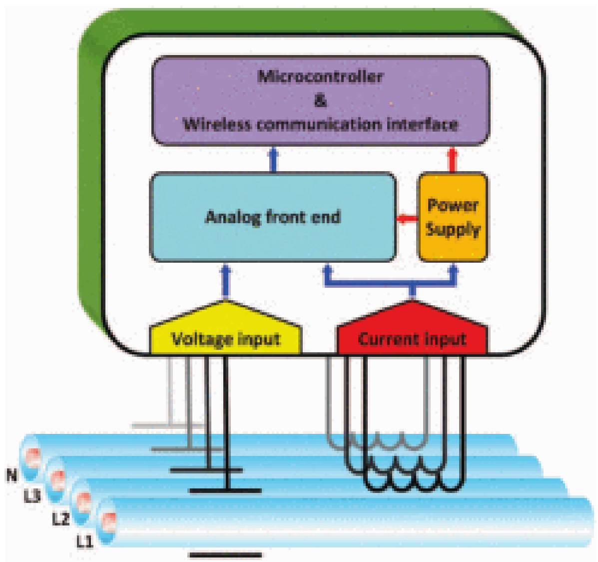

Figure 2.7: The block diagram of a three-phase meter [16]

The power monitoring which follows the mixed signal architecture (i.e. sensors) including the current, the voltage measurements, and the digital processing signal is able to represent the time and frequency analysis energy. It was reported that the low-cost smart meters demonstrated the similar high performance with a maximum 3% deviation to the standard measurement.

In other work, It was reported a single sensor which can measure both voltage and current signal on a type of cable for the domestic applications as the installing prototype in Figure 2.8. The flexible non-invasive power sensor, which provided as the good proximity, was for the accurate electric voltage and current sensing on a standard SPT-2 18AWG as Zip-cord power line. However, due to the materials and production process, the cost was relatively high and the sensor can use with only one type of the cable. The authors designed the voltage and current sensor with 100µm-thick flexible PET substrate. In addition [18], with the coil combing of 50 turns with two sensing electrodes in the space of 1.3x1cm^2 the power sensor exhibited the sensitivity of 31.1µV per 1A, current, and 98.9mV per 115V, voltage respectively. This sensor is detected 60Hz electric standard [18].

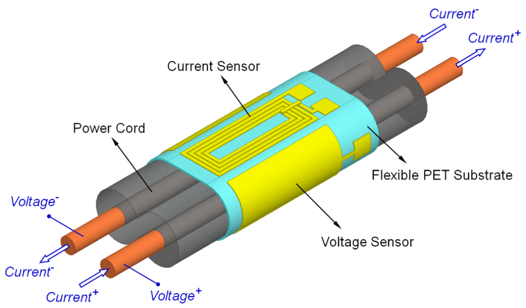

(a)

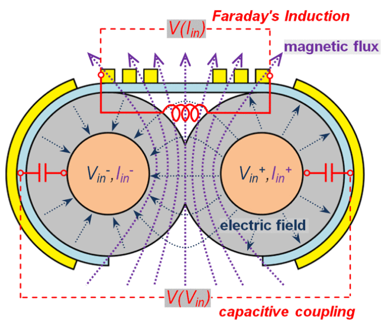

(b)

Figure 2.8: (a), The flexible power sensor and (b), The cross-sectional view [18]

According to [19], the principle of measuring voltage without contacting the conductive part is using the stray electric field to sense the voltage through the non-contactless parasitic capacitance on the high voltage cable. These parasitic sensors were installed as shown in Figure 2.9. The authors also designed this sensor as electric and magnetic fields onto 1 cm by 2 cm printed circuit board (the “Analog” board). Moreover, the authors proposed 4 analog boards in order to measure the electric and magnetic fields at four different points. All of the sensors are connected to an ARM microcontroller via USB connection to a computer. The comparison illustrated the conventional power measurements and the contactless power measurements agree to be better than 1% over the dynamic range of 1000W.

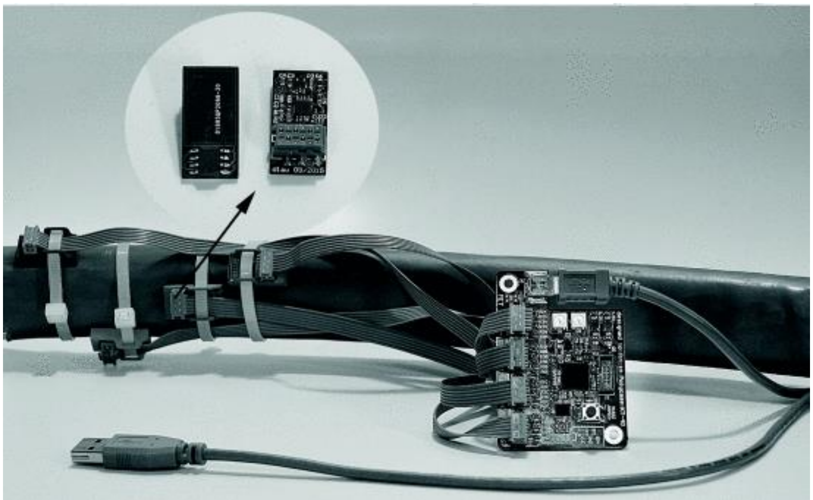

Figure 2.9: The parasitic capacitive sensors wrapped on the high voltage cable [19]

CHAPTER 3
MATERIALS AND METHODS

3.1. Materials

3.1.1. Copper Plate

The copper plate has the best electrical conductivity, both electrical and thermal. The copper plate is also the good electrical conductivity as well as a resistance. Every electrical current were flown through to every metal, however, they still have some resistance, and the current needs to be pushed (by a battery) in order to keep flowing. The current can flow easily through the copper material because of its small electrical resistance, without much loss of energy. This is why the copper material is used in the main cables such as overhead and underground. By the way, many overhead cables tend to use aluminum but this material has less dense than copper. It means that copper is the best choice [20]. We applied 0.2mm of copper plate thickness with 1.25cm length as the voltage sensor (see Figure 3.1). By the way, applying 0.2mm of copper plate thickness is easy to wrap around the cables. The more thickness and length were increased the more capacitance values were bigger. In short, we have to design a capacitive sensor as small as possible.

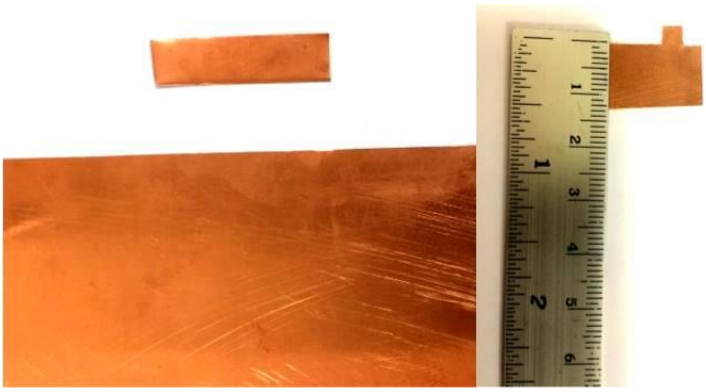

Figure 3.1: The copper plate

3.1.2. LF351N Single Op-amp

The LF351N as shown in Figure 3.2 is Junction gate Field-effect transistor (JFET) input operational amplifier with an internally compensated input offset voltage. This JFET input device provides wide bandwidth, 4MHz, low input bias currents, 50pA, and offset current, 25pA, respectively. We used this JFET to convert voltage and current waveform, which will be discussed in 4.3.

Figure 3.2: The LF351N JFET

3.1.3. MCP3901 Evaluation board 16bit MCU

The MCP3901 ADC evaluation board [21] is launched from Microchip Company as shown in Figure 3.3. It utilized to perform all the measurements in the energy meter. It provides with a development platform for 16-bit PIC® MCU-based applications, coming with existing 100-pin plug-in Module (PIM) system. By the way, this firmware for this board came with a built-in firmware dsPIC33FJ256GP710 PIM module that communicates with the LabVIEW™ software Graphic User Interface for data exchange and the ADC set up.

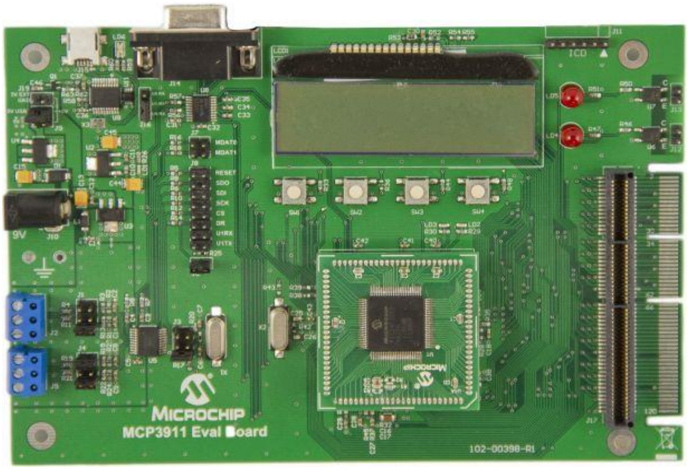

Figure 3.3: The MCP3901 Evaluation Board [21]

The evaluation board comes with a dual MCP3901 ADC output using USB cable (or serial communication) to PC software interface. It comes with 4 ksps at 98dB SINAD and the top speed of 55 ksps that performs on a dual channel ADC. The MCP3901 ADC performs the system through the graphical PC software interface such as the noise with histogram, frequency, the time-domain scope plot, and the statistical numerical analysis. The MCP3901 ADC also supports the input voltage $1V_{p\text{-}p}$. In short, the MCP3901 Evaluation board, built-in with PC firmware that can measure the voltage and current waveform by using MCP3901 ADC.

3.1.4. Software Overview

The MCP3901 ADC Evaluation board comes with the Graphical User Interface (GUI) displayed on a personal computer that performs such as the ADC configuration, the Data analysis for easier system debugging, and the evaluated device board as depicted in Figure 3.4. This MCU board cooperates with MCP3901ADC, which is digitized the quality of charge integrated by a modulator loop as a quantizer. The quantizer is the block performing the analog-to-digital conversion. By the way, this evaluation board can also view and calculate the sensor waveform as frequency and the total harmonic distortion (THD), and the signal to noise and distortion (SIND).

Figure 3.4: The GUI interface of the MCP3901 Evaluation Board

3.2. Methods

3.2.1. Current Sensing Section

The current transformer is one of the main parts of power-measurement circuit design. Non-intrusively, the current can be measured by the electromagnetic field radiated from the wire without any interruption or cutting. It is convenient and safe to install. In this work, we exploit the noninvasive current transformer to obtain the current waveform as shown in Figure 3.5.

Figure 3.5: The current transformer [22]

We can find a turn ratio of this ideal current transformer [23] as follows:

$$a = \frac{N_P}{N_S} = \frac{I_S}{I_P} = \frac{V_P}{V_S} \tag{2}$$

Where a is turns ratio of a transformer, N_P, primary turns, N_S secondary turns, I_S, secondary current, I_P, primary current, and V_P, primary voltage while V_S is secondary voltage, respectively. In this work, the current transformer used in our prototype is SCT-013-030 [22], available on market, with built-in burden resistor.

3.2.2. Voltage Sensing Section

The voltage signal is crucial for calculating the active power (W) and the apparent power (VA), and power parameters such as the power factor (PF). This parameter requires precise voltage measurement in order to obtain the correct voltage information. The conventional voltage measurements techniques in the AC power line require electrical connecting to the conductive wires inside the power cord. In contrast to the conventional methods, we proposed a contactless voltage measurement consist of a small-thickness copper plate film wrapped around the insulating sheets of the cable. The capacitive coupling (capacitive voltage sensors) wrapped between the internal conductive element of the wire and the external are used. These sensors can generate the electrical field by line and neutral cable. Thus, the sensors obtain as current in response to the drifting voltage because the coupled voltage sensors obtain the voltage waveform from part of each cable through the external insulation of the system as shown in Figure 3.6.

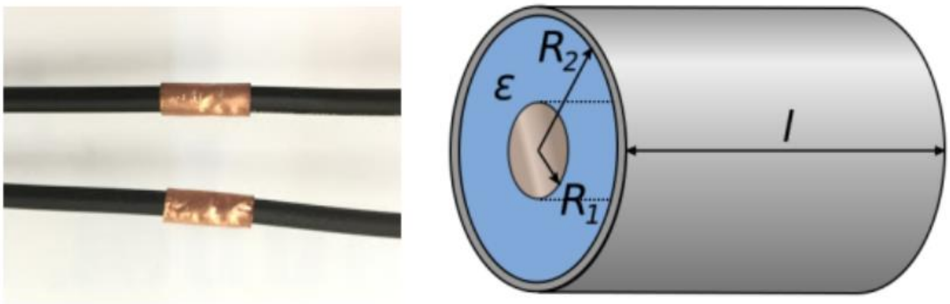

Figure 3.6: The capacitive coupling sensor [24]

We obtained a cylindrical capacitor situated between the inner side of the copper plate of radius R_2 and the surface of the conductive wire of the cable for radius R_1. The insulating cable comes with permittivity ε separates these radii. We can calculate the capacitance value between the two conductors of such structure given by following [25]:

$$C_{Sensor} = \frac{2\pi\varepsilon l}{\ln \frac{R_2}{R_1}} \qquad (3)$$

The issue statement consists of equations, which provide to obtain the unknown of two parameters: C_{sensor} and V_{in}. These two equations are calculated with the transfer function of two identical filters. We choose to calculate the process of the analog front-end (see Figure 3.7).

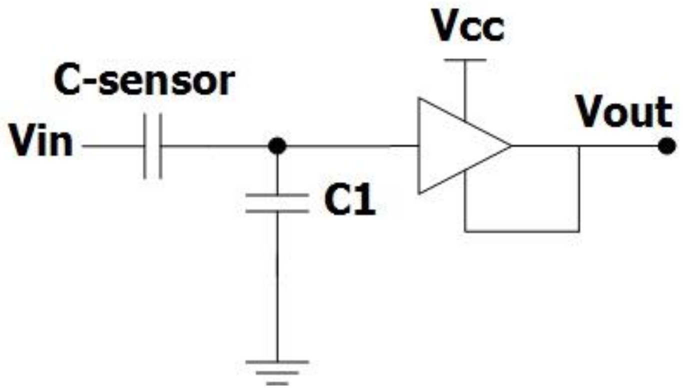

Figure 3.7: The capacitive voltage sensor front-end

The filter as illustrated in Fig. 17 is a voltage divider for the AC signal made of two capacitors: the capacitor, C_{sensor}, whilst precision capacitance C_1 was chosen as 470pF by regarding the value of the two capacitors. The output relationship of this filter is illustrated as the formula:

$$V_{out} = \frac{C_{sensor}}{C_{sensor} + C_1} V_{in} \qquad (4)$$

Where C_{sensor} is the capacitive coupling and C_1 is the precision capacitor. In addition, the analog front end converted the signal from both filters (voltage divider) through the input of ADC by using the differential amplifier as shown in Figure 3.8.

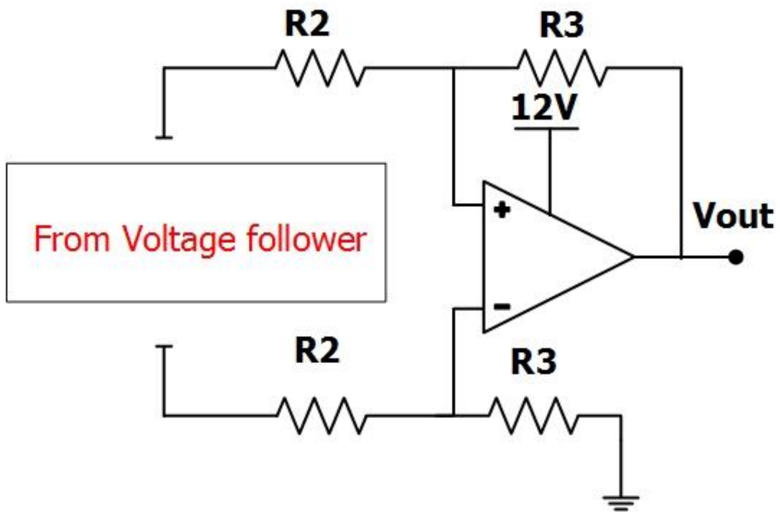

Figure 3.8: The differential amplifier

Then the output voltage of the differential amplifier is calculated by following formula:

$$V_{out} = \frac{R_3}{R_2} V_{in} \tag{5}$$

Where R_3 of 20kΩ and R_2 of 1kΩ is the precision resistances. The whole circuit designed of the analog front end is shown in Figure 3.9. By Eq.5, the gain of the differential amplifier (V_{out}/V_{in}) is 1/20.

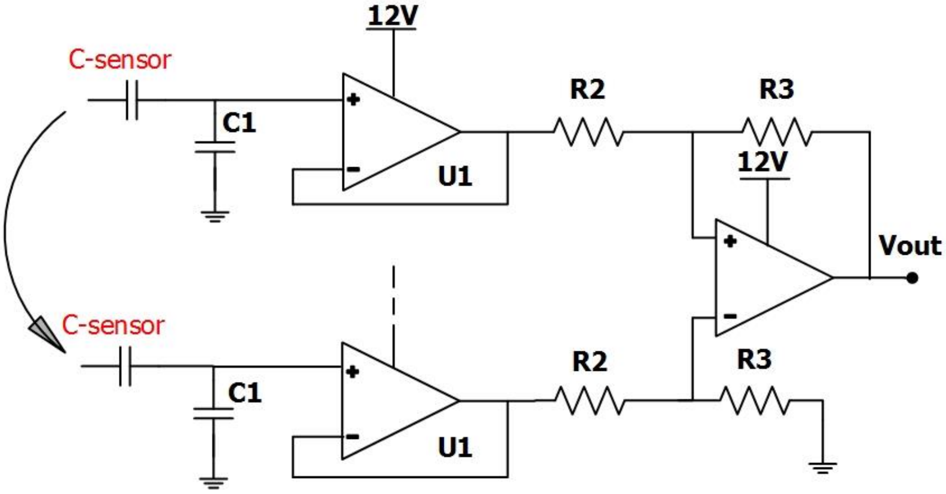

Figure 3.9: The analog front-end circuit

Once the value of C_{sensor} is known, the calculation of V_{in} can be performed by using Eq.6. To appropriately measures AC voltage from a power line, C_{sensor} and C1 should be chosen to result in a ration that defines V_{out} in the range of operating voltage of the analog front-end circuit.

$$V_{in} = \left(1 + \frac{C_1}{C_{sensor}}\right) V_{outCC} \tag{6}$$

3.2.3. Power Features Calculation

The expressions for the root mean square (rms) value is obtained as following [26]:

$$V_{rms} = \frac{V}{\sqrt{2}} \tag{7}$$

$$I_{rms} = \frac{I}{\sqrt{2}} \tag{8}$$

Hence, real power consumption is illustrated, as follows:

$$P = V_{rms} * I_{rms} * \cos\theta \tag{9}$$

The phase angle of the load impedance plays a key role in the absorption of power by the load impedance. To recognize the importance of this factor in the AC power computations, the term $\cos(\theta)$ is referred to as the power factor (PF). Hence, the expression for the power factor is illustrated as following:

$$PF = \cos(\theta) = \frac{P}{V_{rms} I_{rms}} \tag{10}$$

Where V_{rms}, rms voltage value, and I_{rms}, rms current value of the load, respectively. Incidentally, power factor (PF) also can also be investigated with the phase shift offset as the period of the reference signal 20ms for 360 degrees. The phase shift offset will be discussed in section 4.3.

CHAPTER 4
EXPERIMENTAL SETUP

4.1. Current Measurement

SCT-013-030 transformer is used to convert current to voltage. This current sensor performs a noninvasive measurement so we clamp it on the line cable side as shown in Figure 4.1. The line and neutral cables are connected to a 220VAC 50Hz power line source. The line and neutral cables are connected to the power line source, which employs a 200W tungsten lamp. Its main electrical characteristic is the maximum output voltage of 1V, which response to the maximum input current 10A as a specification in [22].

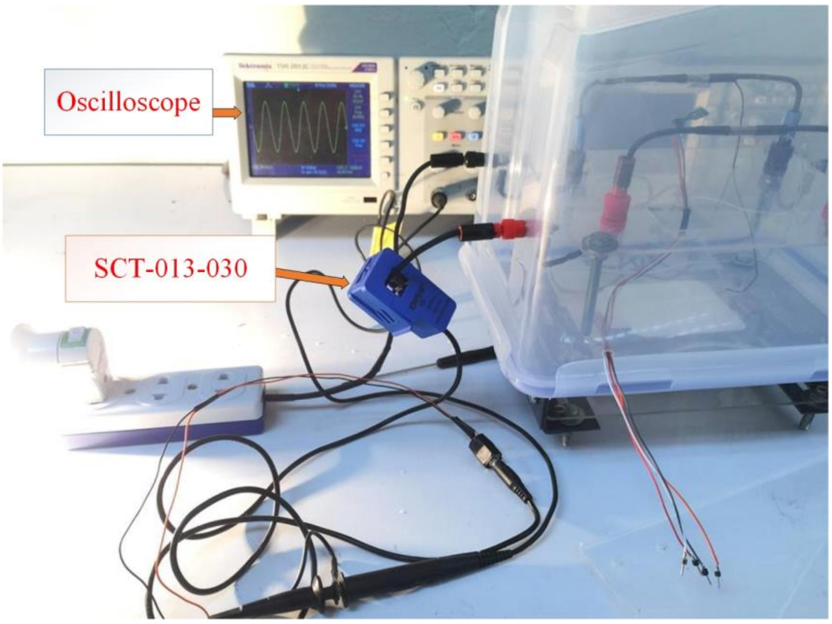

Figure 4.1: The current sensor installation

Figure 4.2 has illustrated the experimental set-up obtains 90.5mV on the Oscilloscope with 0.905A as calculated in 3.2.1. The blue color is the current waveform signal measured by the current transformer and the orange color is the output of the proposed voltage system.

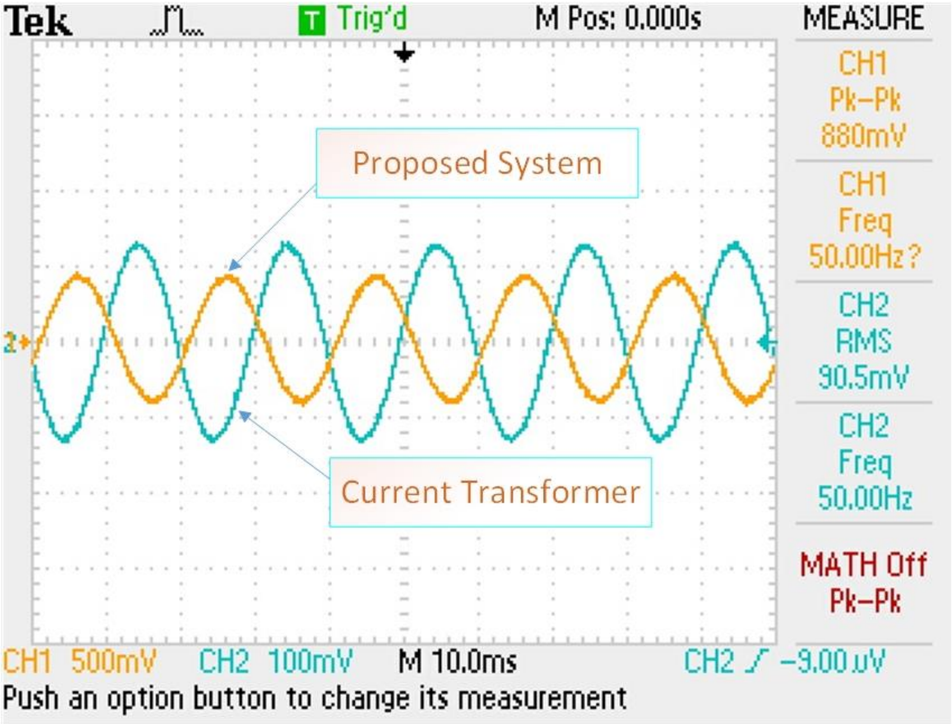

Figure 4.2: The current waveform displayed data

4.2. Capacitance Characteristic Measurement

4.2.1. Capacitor Measured with LCR Meter

A copper sheet of dimension (l=1.25cm-length) wrapped around the side of cable standard TI 11-2531 cable. In the preliminary study, the direct measurement of the capacitance value C_{sensor} is used the LCR HITESTER HIOKI 3551 with the set-up illustrated in Figure 4.3. With this LCR meter, the capacitance value C_{sensor} is identified as 7.55pF (see Figure 4.4-4.5).

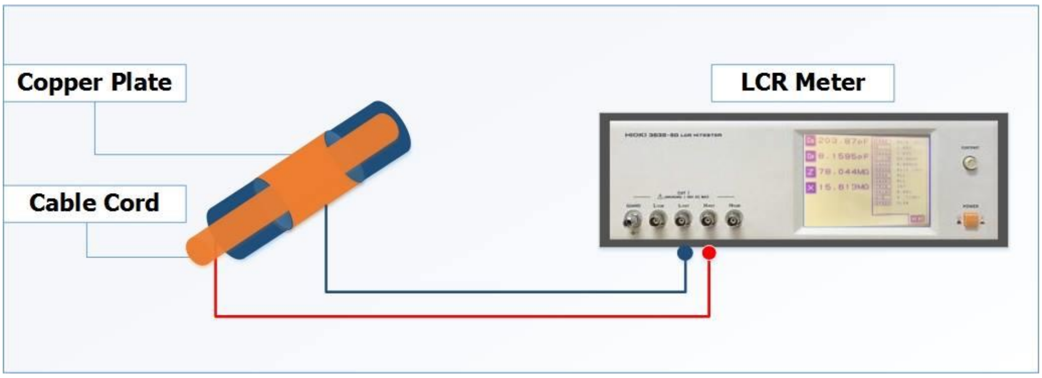

Figure 4.3: The prototype of the copper plate measure with the LCR meter

Figure 4.4: The copper plate clipped with LCR’s clipper

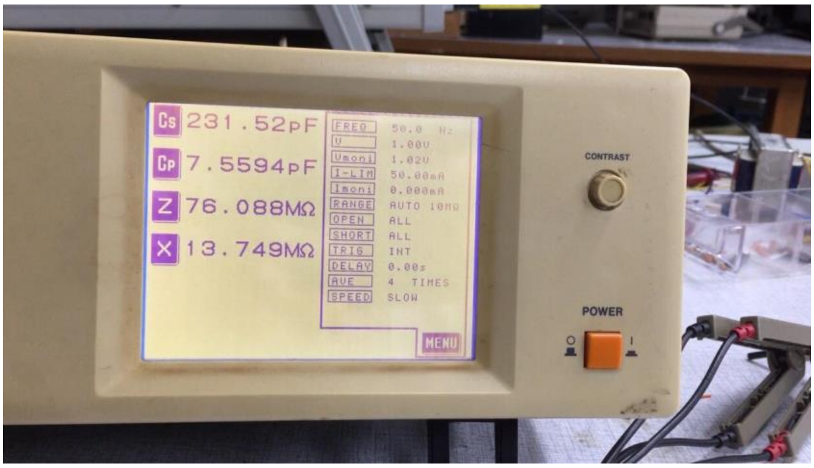

Figure 4.5: The capacitance value obtained by LCR meter

The LCR meter measurements are also connected with 1V AC 50Hz voltage reference (see Figure 4.6). The capacitive sensors clip with clipper of the LCR meter as mentioned in Figure 4.4. The capacitance values are also changed while measuring with LRC meter in 30 minutes.

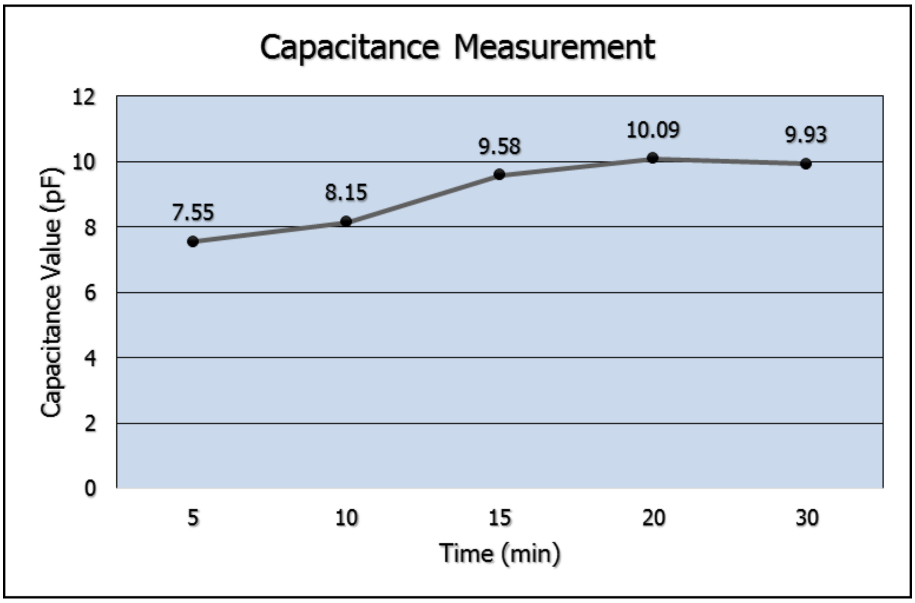

Figure 4.6: The capacitance value shifted with the LCR meter

4.2.2. Sensor Output Voltage Drift for Calibration

The cable is wrapped with a copper plate sheet of dimension (l=1.25cm length). The copper plate, namely the capacitive sensor, soldered to the precision capacitor (C_{pre} =12pF), illustrated in Figure 4.7.

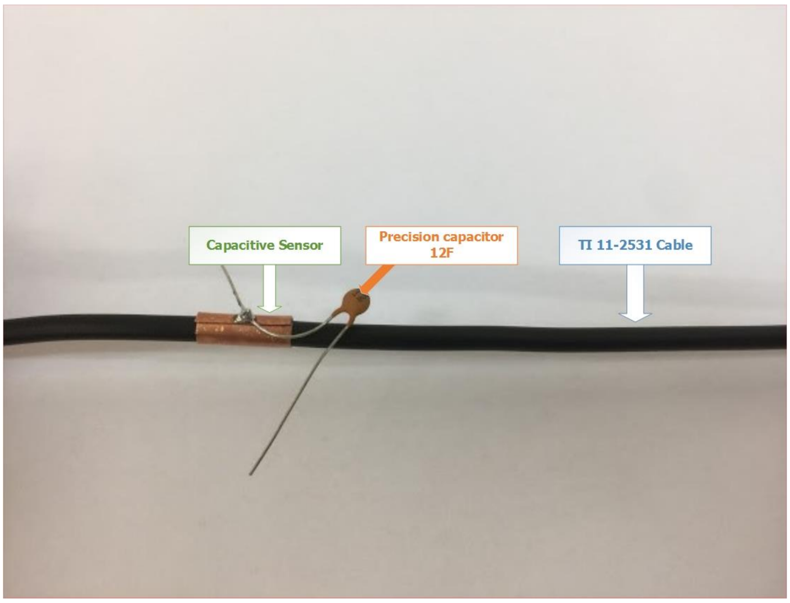

Figure 4.7: A capacitive sensor soldered with the precision capacitor

The capacitive installed with the LCR meter, the Oscilloscope, and the function generator as illustrated in Figure 4.8. The voltage amplitude of the function generator is varied from 5V to 15V in 9 samples. The experiment results were obtained the changing of capacitance value as shown in Figure 4.9. While we supply 5V, the capacitance values are varied from 2.71nF to 6.55nF. The capacitance values change from 2.69nF to 6.86nF when we supply 10V. Moreover, by supply 15V the capacitance values are varied from 2.69nF to 6.86nF

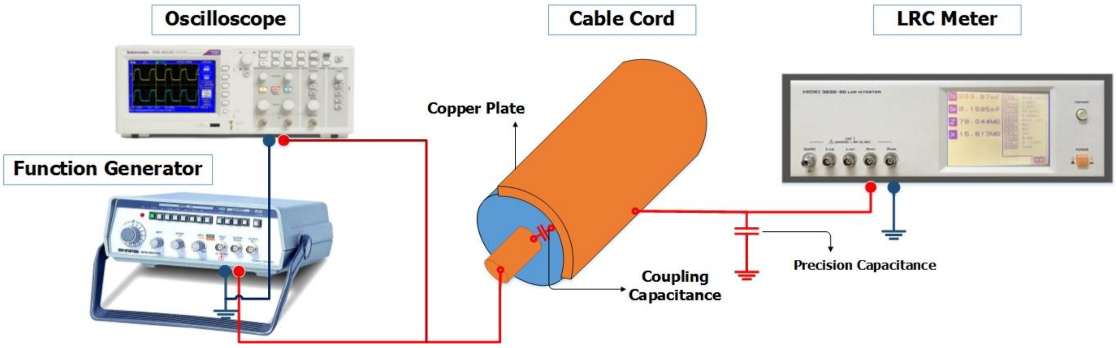

Figure 4.8: Prototype of the capacitor with equipment meters

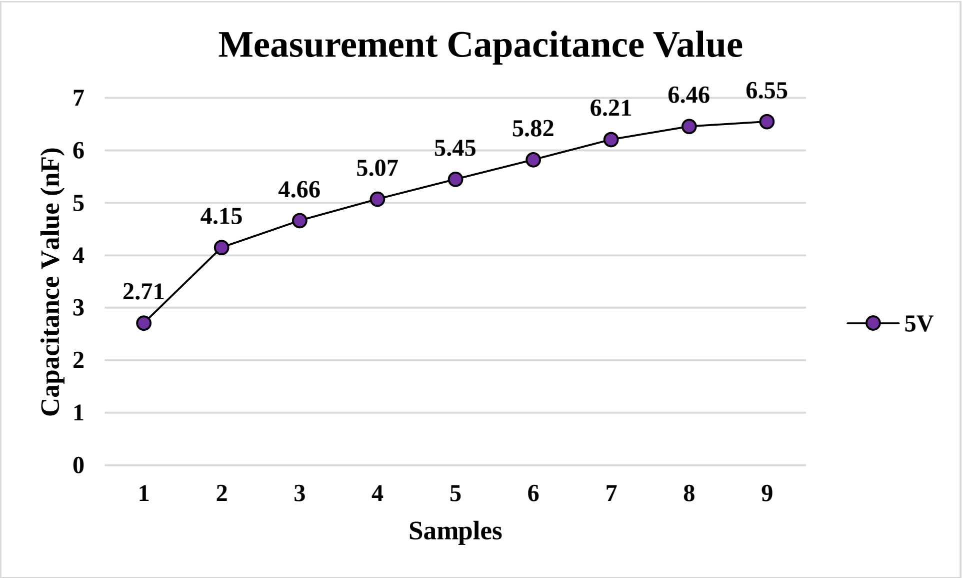

a). The capacitance values obtained with 5V supply

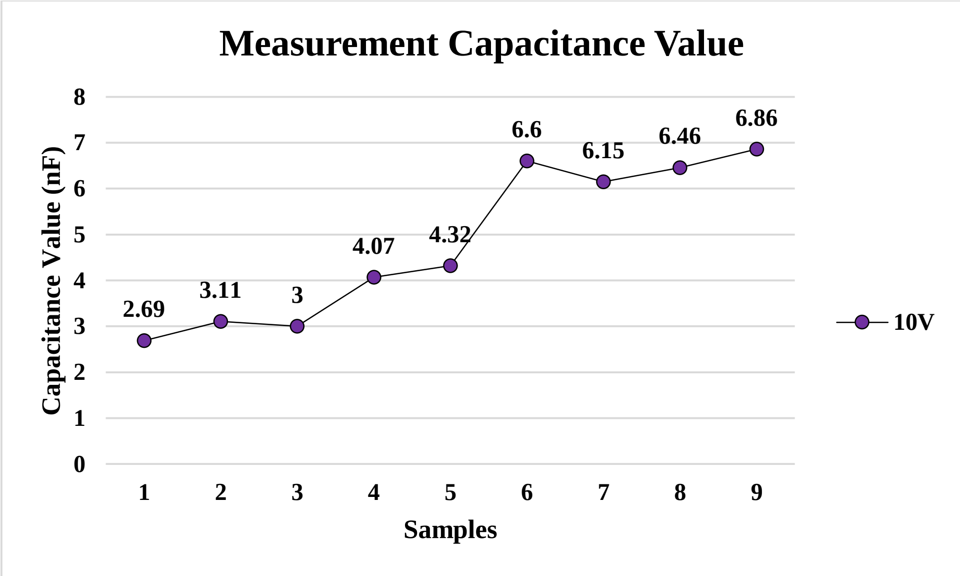

b). The capacitance values obtained with 10V supply

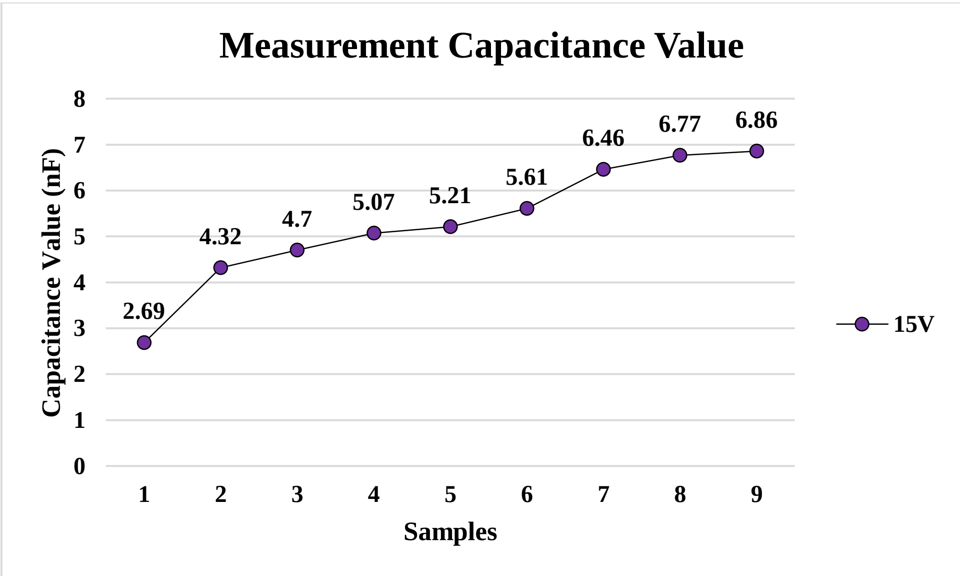

c). The capacitance values obtained with 10V supply

Figure 4.9: The capacitance values obtained from the varied voltage

4.2.3. Capacitive Sensor with Voltage Buffer

Figure 4.10 has illustrated the capacitor sensor and the precision capacitor obtained the capacitance data using the LF353 JFET as the voltage follower. The Line and Neutral of the function generator is a 10.4_{Vp-p} AC 50Hz connected to cable and on the other sides, the LF353 JFET connected to the capacitive sensor by the load, which employ with the 100Ω of the precision resistance.

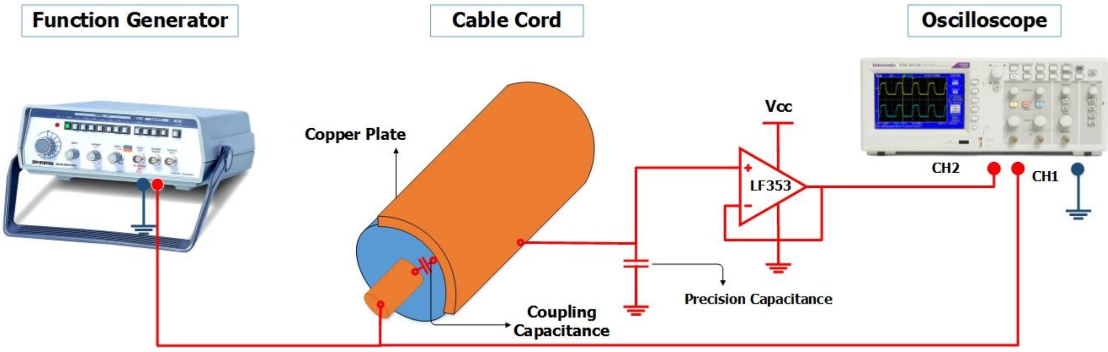

Figure 4.10: The prototype of the capacitive sensor connected to the LF353

The experimental result of measured V_{out} is illustrated in Figure 4.11. The result has shown that V_{out}=4.04V_{p-p}. It can examine that the capacitor sensor can measure by using a copper plate sensor.

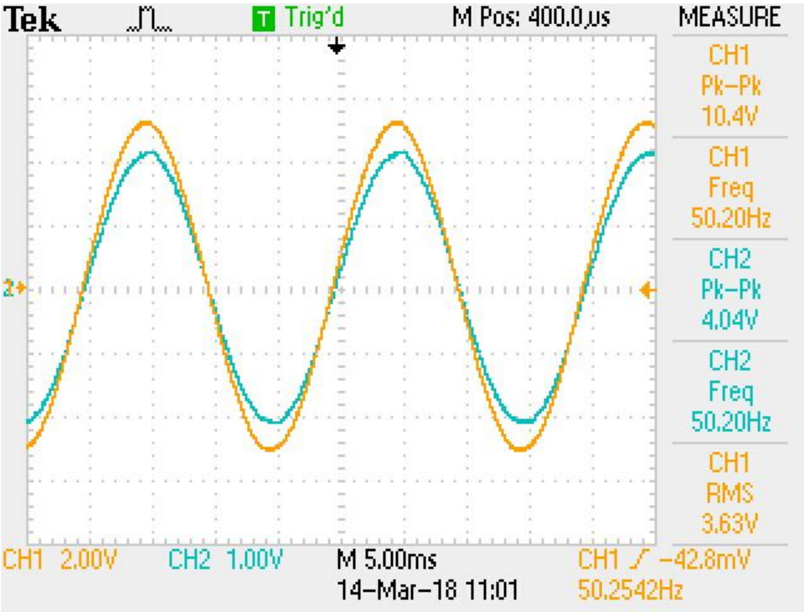

Figure 4.11: The result of the capacitive voltage sensor with a voltage buffer

4.2.4. Capacitor Sensor with Instrumentation amplifier (IA)

The advantage of the three op-amps provided the ability to reject common-mode signal components i.e. noise or undesired DC offsets) while amplifying the differential-mode components. The three op-amps (Operational Amplifier) were connected to both sides of the voltage followers, which connected with the capacitive sensor (see Figure 4.12).

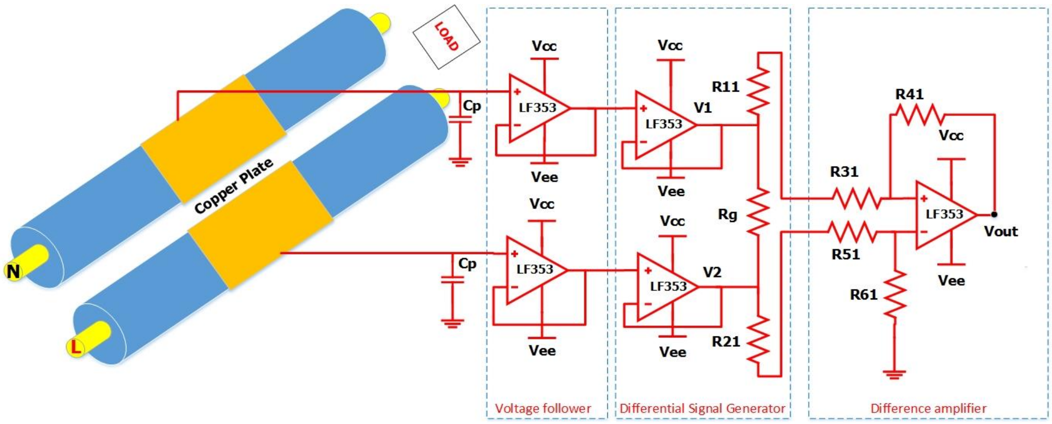

Figure 4.12: The prototype of the capacitive sensor attached with IA

For the primary study, the voltage output obtained $11.8V_{p\text{-}p}$, with gain=3 from both sensors are given as shown in Figure 4.13 while the function generator provided $10.06V_{p\text{-}p}$. The results have shown that the capacitive waveform can reject noise and DC offsets and testing signal condition.

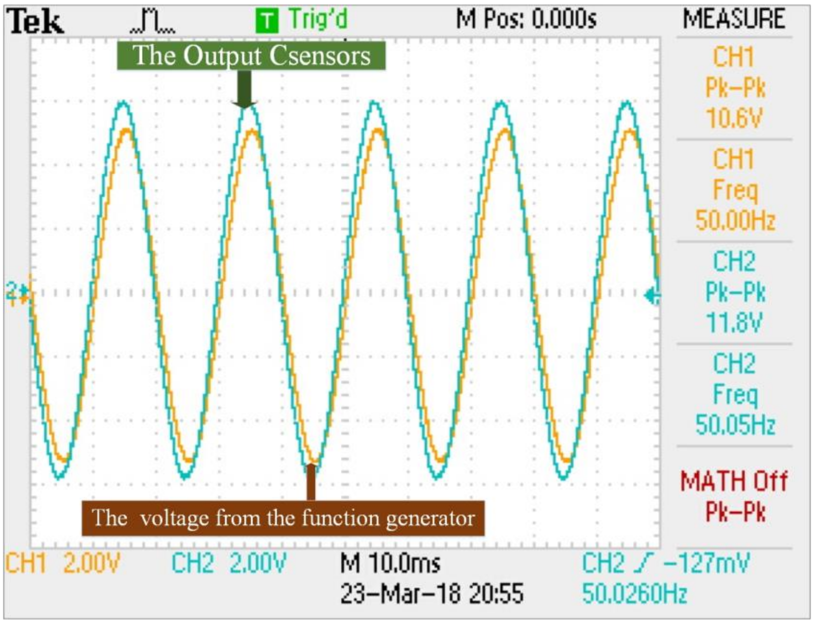

Figure 4.13: The results from IA study

4.2.5. Humidity and Temperature Effects

The humidity and temperature of capacitive coupling sensors, namely voltage sensors, are measured by SHT11, a single chip relative humidity, and temperature sensor. The humidity and temperature values have calibrated the data with Arduino MEGA 2560 using the embedded software. Figure 4.15 and Figure 4.16 illustrates the measurement of capacitance drift caused by humidity and temperature. The experimental results of the sensor output voltage value obtained from testing 128 sample values (see Figure 4.17), which are given average value such as 0.58% of humidity, 27.8℃ of temperature, and voltage 481mV of voltage. When the humidity and temperature are increased the capacitance value is also increased. As the results, it can be concluded that the voltage value shifts 1% as compared to the voltage result as mentioned in 4.3.

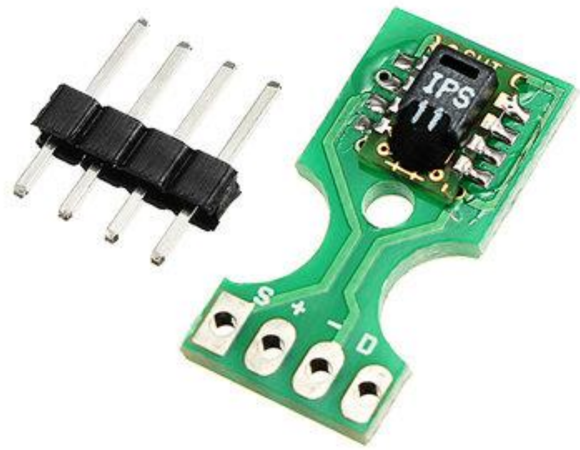

Figure 4.14: The SHT11 sensor

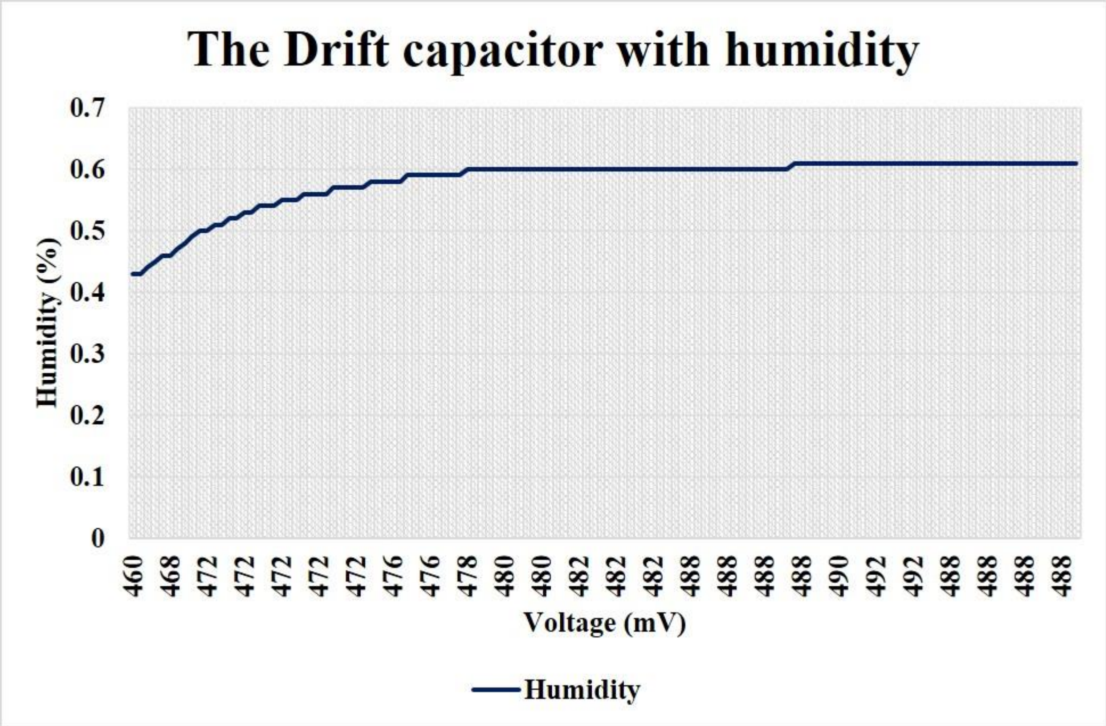

Figure 4.15: The drift capacitive voltage sensor with humidity

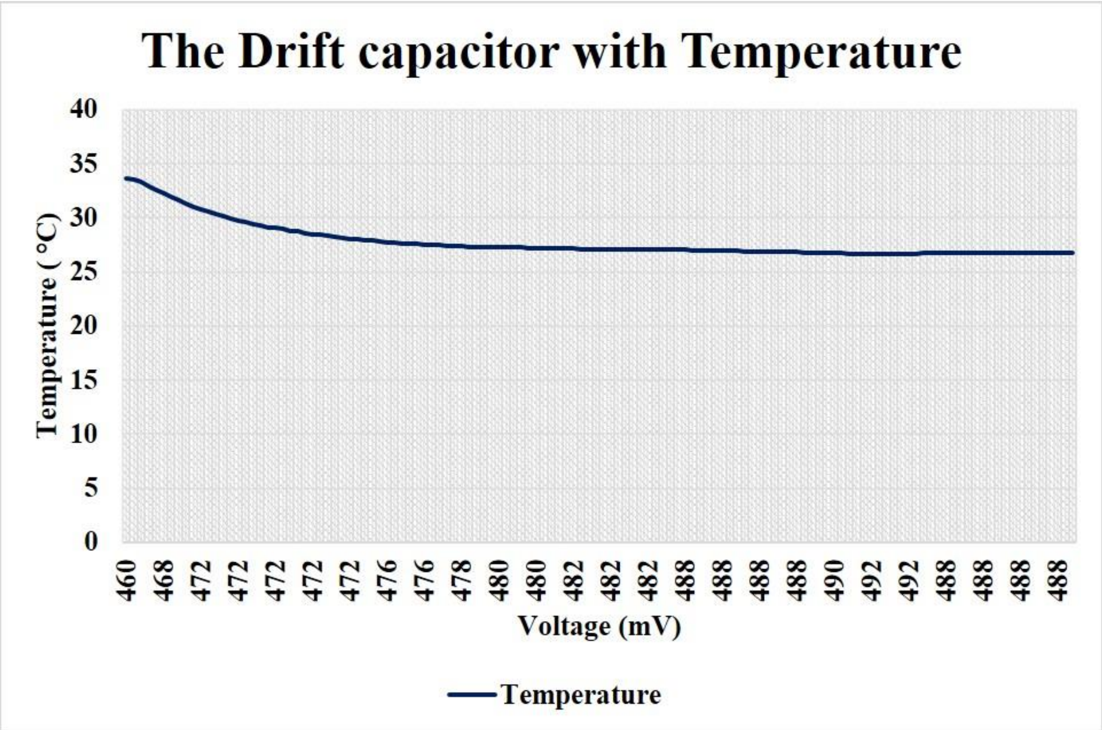

Figure 4.16: The drift capacitive voltage sensor with temperature

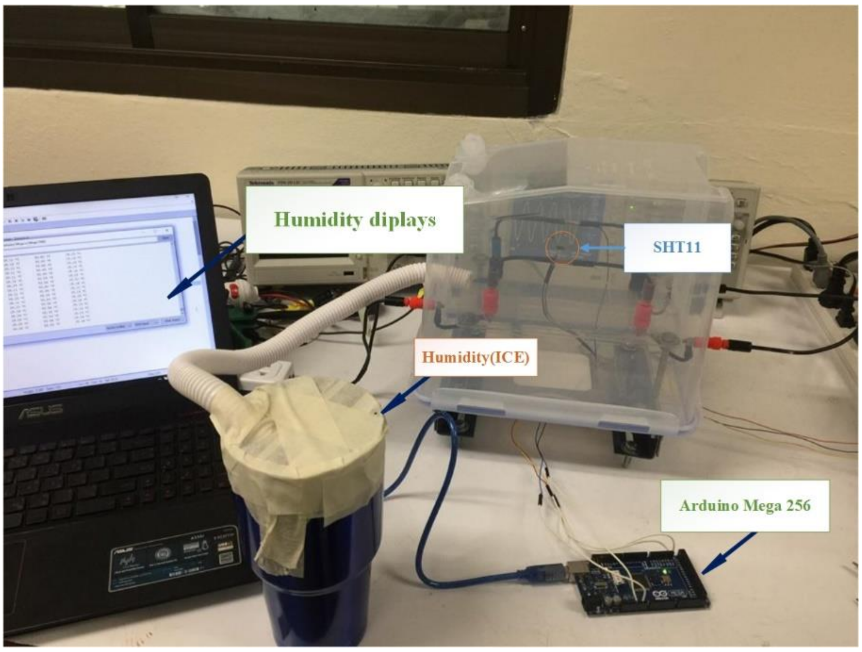

Figure 4.17: Humidity and temperature measured by SHT11

4.3. Implementation of Proposed System

To evaluate our hypothesis and the performance of the proposed design, we implemented the proposed system of voltage sensor as shown in Figure 4.18. A pair of copper sheets (l=1.25cm-length) is wrapped around both sides of the line and neutral as the TI 11-2531 cables. Once both capacitive sensors connected to precision capacitor C1, displays as 471pF by regarding the value of the two capacitors. The voltage divider ratio is 0.02 (V_{outCC}/V_{in}).

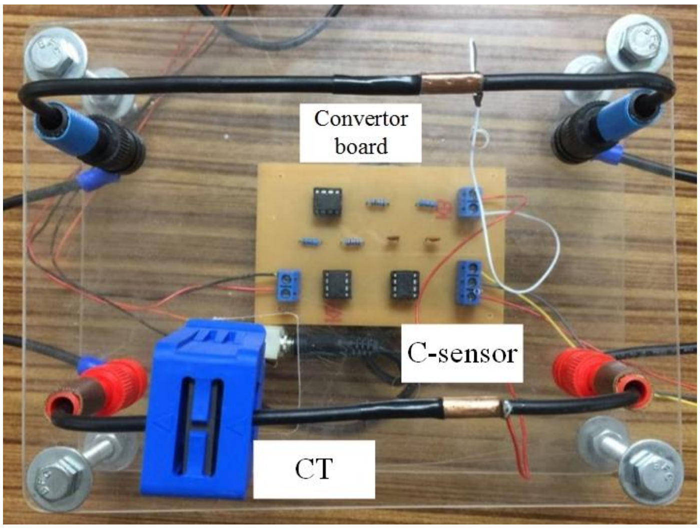

Figure 4.18: The proposed system installation

Both sensors are connected to the input of the analog front-end, and the oscilloscope to monitor the output voltage V_{out}. Moreover, we connected the current transformer at the line cable as discussed in 4.1. Its output is connected to another channel of the oscilloscope. The line and neutral cables are connected to a 220V AC 50Hz power line source at one side and the other side connected to the resistive load, which employs a 200W tungsten lamp (see Figure 4.19).

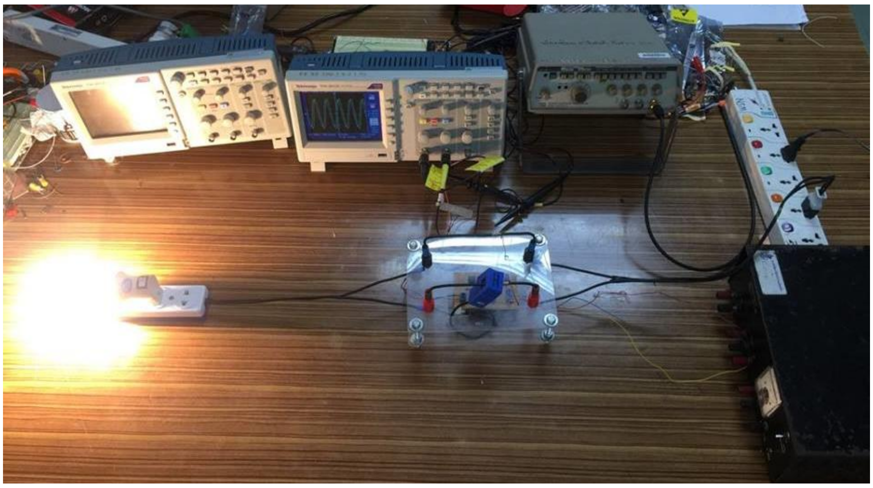

Figure 4.19: The new proposed system connected with Tungsten lamp 200W

Experimental result of measured V_{out} value is illustrated in Figure 4.20. The results have shown that V_{out} =476m$V_{p\text{-}p}$ with gain =1/20, as mentioned in 3.2.2. By using the backward calculation, we calculated the value of V_{outCC} = 4.76V (impedance buffer). At the same time, we got the value of capacitor sensor 7.33pF. Finally, V_{in} is approximately 220V_{rms} by Eq.6.

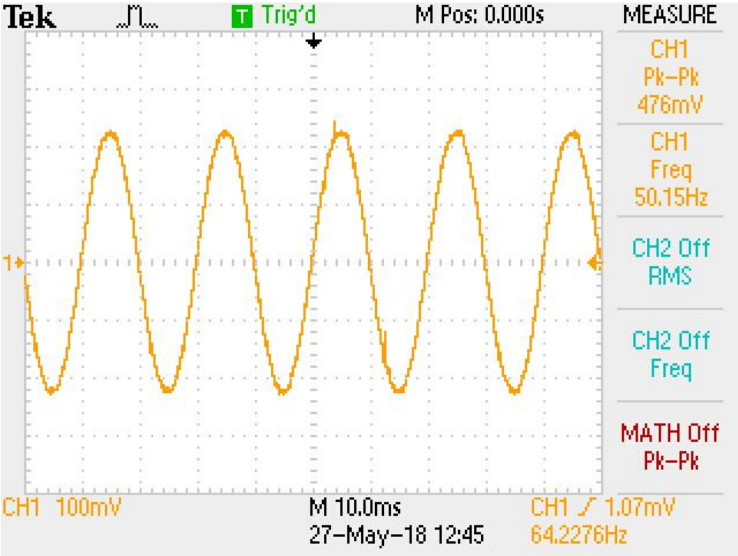

Figure 4.20: Result of the newly proposed voltage sensor

Moreover, we investigated the phase shift offset of the proposed system in comparison with a voltage transformer. The oscilloscope as illustrated in Figure 4.21 shows the result. The output of the proposed system is 900µs. This causes from the behavior of the parasitic capacitance of the sensors. The output of the proposed system used for compensation of the power factor calculation.

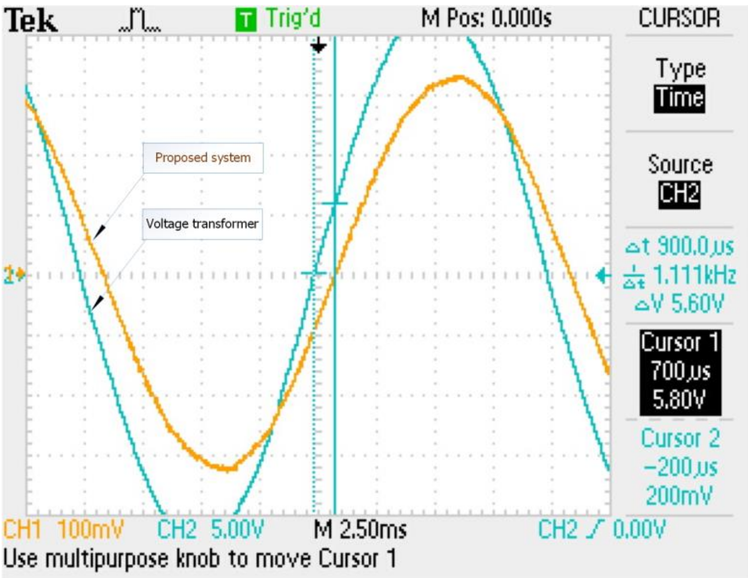

Figure 4.21: Phase shift offsets between voltage transformer and the proposed system

The period of the reference signal is 20ms (from Figure 4.21), thus, the phase shift error between voltage transformer and proposed system is 16.20 degree as Δt is 900μs. The voltage leads current phase shift approximately 27.00 degree as Δt is 1.50mS (see Figure 4.22). Then the active power P and power factor (PF) are obtained as 199.09W and 0.99 respectively based on the voltage and current waveform of our proposed system.

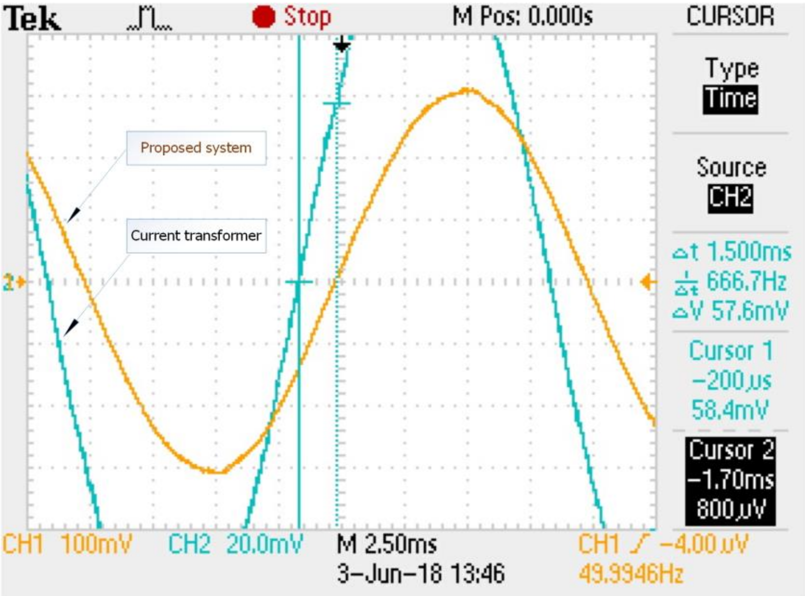

Figure 4.22: Phase shift between current transformer and output voltage

The results have been validated by using a calibrated digital wattmeter providing the active power and the power factor as illustrated in Figure 4.23-4.24. The proposed system demonstrates the capability of measuring power and power parameters with the error of active power estimation approximately 2.5% in comparison with the standard Wattmeter. By using the knowledge of phase shift offset, the compensated power factor determines 0.99, which is the same as the reference value from the Wattmeter.

Figure 4.23: Active power displayed on Wattmeter

Figure 4.24: Power factor measured with Wattmeter

4.4. The Capacitor Drift in the Proposed System

The drift if the capacitive voltage sensor is from the humidity and temperature as mentioned in 4.2.5. The capacitance value changes 1% while the humidity and temperature are increased. The V_{out} is designed for the input of both analog channels of the MCP3901 evaluation board (CH0±, CH1±), while both channels have to acquire voltage input waveform only ±1V 50Hz. The Figure 4.25 is illustrated the capacitance value calculated V_{out} from 350mV to 1V within 9 samples were chosen during in three days. Thus, we can obtain the varied capacitive value with the voltage waveform. The results have shown the capacitance varied from 350mV, 5.35pF to 1V, 15.61pF respectively. In short, the varied capacitance values are affected based on some conditions such as environment, humidity, temperature and noise signal.

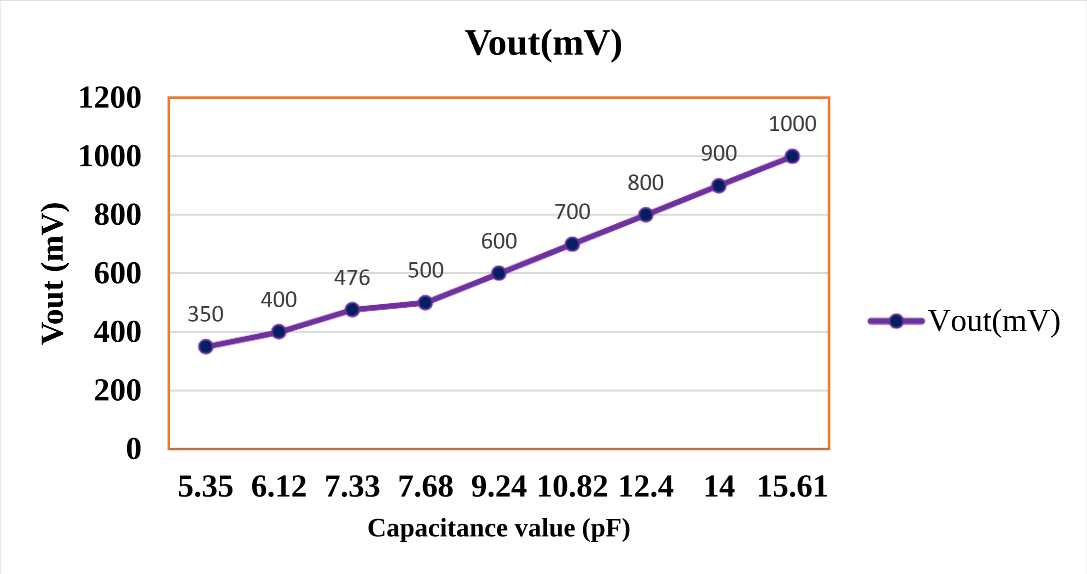

Figure 4.25: The drift of the capacitive voltage sensors

4.4. Monitoring Waveform with GUI

Figure 4.26 illustrated the voltage and current waveforms of the proposed system monitored by Graphic User Interface (GUI). The voltage and current waveform input to pins of MCP3901 ADC presented in GUI interface. The GUI was monitored and calculated data such as both voltage and current waveform with 50Hz of frequency. Furthermore, it also can obtain total harmonic distortion (THD), 13.06dB, signal to noise and distortion (SINAD), 8.22, respectively.

Figure 4.26: The monitoring data viewer (GUI)

CHAPTER 5
CONCLUSION AND SUGGESTION

5.1. Conclusion

We present the low-cost capacitive voltage sensor and current waveform measured without intruding the cable. The nonintrusive manner measures the voltage and current waveform in the single-phase electrical line. In the proposed system, a low-cost capacitive voltage sensor is developed. The advantage of our proposed system is that it does not need cutting or tapping of wire. In our work, it can be concluded that the capacitance value of the sensor (i.e. real calculation and measured with LCR meter) is approximately around 5pF to 15pF with 350mV to 1V respectively. The sensor is used with the analog front end in the simulated power measurement in the experiment. The proposed system achieved accurate power measurement with 2.5% of errors as compared with standard Wattmeter while the sensor measure 476mV.

5.2. Suggestion and Future Work

There are many factors affecting the capacitive coupling such as humidity, temperature, signal frequency, and age of capacitor. However, the humidity and temperature cannot be controlled due to the limitation of equipment. It is suggested that a calibration factor should be dynamically modified related to the environmental effects, i.e. auto/self-calibration to reduce output voltage drift.

The GUI interface of the MCP3901 Evaluation board can monitor some data such as total harmonic distortion (THD), frequency, voltage, and current waveform, and signal to noise and distortion (SINAD). It is suggested that once the GUI interface will be monitoring the voltage and current it should also be able to calculate and obtained the power consumption value.

REFERENCES

[1] G. Hart, "Nonintrusive appliance load monitoring," *Proceedings of the IEEE*, vol. 80, no. 12, pp. 1870-1891, December 1992.

[2] H. Rabab and R. Ghadir, "Survey on Smart Grid," in *Proceedings of the IEEE SoutheastCon 2010 (SoutheastCon)*, 2010.

[3] N. Tamkittikhun, T. Tantidham and P. Intakot, "AC power meter design for home electrical appliances," in *2015 12th International Conference on Electrical Engineering/Electronics, Computer, Telecommunications and Information Technology (ECTI-CON)*, 2015.

[4] B. Demenico, P. Danilo and B. Luca, "A new non-invasive voltage measurement method for wireless analysis of electrical parameters and power quality," in *2013 IEEE SENSORS*, 2013.

[5] S. Kang, S. Yang and H. Kim, "Non-intrusive voltage measurement of ac power lines for smart grid system based on electric field energy harvesting," *Electronics Letters*, vol. 53, no. 3, pp. 181-183, 2017.

[6] B. Campbell and P. Dutta, "Gemini: A Non-invasive, Energy-Harvesting True Power Meter," in *2014 IEEE Real-Time Systems Symposium*, 2014.

[7] R. M. Ramyar , F. Alan, M. Farah and R. Kaamran, "A survey on Advanced Metering Infrastructure," *International Journal of Electrical Power & Energy Systems*, vol. 63, pp. 473-484, December 2014.

[8] E. Spano, L. Niccolini, S. Di Pascoli and G. Iannaccone, "Last-Meter Smart Grid Embedded in an Internet-of-Things Platform," *IEEE Transactions on Smart Grid*, vol. 6, no. 1, pp. 468-476, January 2015.

[9] S. S.-u. Hasan Rohani, A. L. Awan, S. Akhtar, and H. Ansari, "Smart grid system," in *2016 SAI Computing Conference (SAI)*, 2016.

[10] X. Fang, S. Misra, G. Xue and D. Yang, "Smart Grid #x2014; The New and Improved Power Grid: A Survey," *IEEE Communications Surveys Tutorials*, vol. 14, no. 4, pp. 944-980, 2012.

[11] M. Clive, B. John, L. M.A., B. W., L. Andrew, S. Ron, S. Keith, W. Time, T. Mike, M. Luis, D. Izzat, K. Walt, B. Alan and W. DF, Electrical Engineering - Know it All, Elsevier, 2008.

[12] P. Donald, "Electrostatic voltmeter and fieldmeter measurements on GMR recording heads," in *Electrical Overstress/Electrostatic Discharge Symposium Proceedings 2000 (IEEE Cat. No.00TH8476)*, 2000.

[13] T. K.M. and C. W.L., "Dual capacitive sensors for non-contact AC voltage measurement," *Sensors and Actuators A: Physical*, vol. 167, no. 2, pp. 261-266, 1 June 2011.

[14] C. Villani, D. Balsamo, D. Brunelli and L. Benini, "Ultra-low power sensor for autonomous non-invasive voltage measurement in IoT solutions for energy efficiency," in *Smart Sensors, Actuators, and MEMS VII; and Cyber Physical Systems*, 2018.

[15] D. Brunelli, C. Villani, D. Balsamo and L. Benini, "Non-Invasive voltage mesurement in a three-phase autonomous meter," *Microsystem Technologies,* vol. 22, no. 7, p. 1915–1926, 2016.

[16] C. Villani, S. Benatti, D. Brunelli and L. Benini, "A contactless three-phase autonomous power meter," in *2016 IEEE SENSORS*, 2016.

[17] C. Villani, S. Benatti, D. Brunelli and L. Benini, "A Contactless, Energy-Neutral Power Meter for Smart City Applications," in *International Conference on Applications in Electronics Pervading Industry, Environment, and Society*, 2017.

[18] C. Yung-Chang, H. Wie-Hung, C. Shih-Hsien and T. C. Yu, "A Power Sensor Tag With Interference Reduction for Electricity Monitoring of Two-Wire Household Appliances," vol. 61, no. 4, pp. 2062-2070, 2014.

[19] D. Lawrence, J. S. Donnal, S. Leeb and Y. He, "Non-Contact Measurement of Line Voltage," *IEEE Sensors Journal*, vol. 16, no. 24, pp. 8990-8997, December 2016.

[20] "Copper Development Association (CDA)," 17 06 2018. [Online]. Available: http://copperalliance.org.uk/education/education-resources.

[21] "The-MCP3901-Evaluation-Board-16bits-MCU", 2018. [Online]. Available: http://www.microchip.com/.

[22] "SCT-013-030", 2018. [Online]. Available: https://www.arduinoall.com/.

[23] S. Md.Abdus and M. Quazi, Power Systems Grounding, Springer, 2016.

[24] Cylindrical-Capacitor, 2018. [Online]. Available: https://electronicspani.com/.

[25] B.L.Theraja, A.K.Theraja, and S.G.Tarnekar, A Textbook of Electrical Technology, 2005.

[26] R. Giorgio, Principles and Applications of Electrical Engineering, 2003.

[27] P. Danilo , B. Domenico , B. Davide and P. Giacomo, "Perpetual and low-cost power meter for monitoring residential and industrial appliances," in *2013 Design, Automation Test in Europe Conference Exhibition (DATE)*, 2013.

[28] S. Grisha and K. Nikolay, "Measurement of Temperature and Humidity using SHT 11/71 intelligent Sensor," *Bulgaria: Technical University,* 2004.

APPENDIX A

Catalog of LF351N

FAIRCHILD SEMICONDUCTOR®

www.fairchildsemi.com

LF351

Single Operational Amplifier (JFET)

Features

- Internally trimmed offset voltage: 10mV
- Low input bias current : 50pA
- Wide gain bandwidth : 4MHz
- High slew rate : 13V/μs
- High input impedance : $10^{12}\Omega$

Description

The LF351 is JFET input operational amplifier with an internally compensated input offset voltage. The JFET input device provides wide bandwidth, low input bias currents and offset currents.

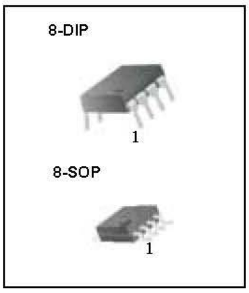

Internal Block Diagram

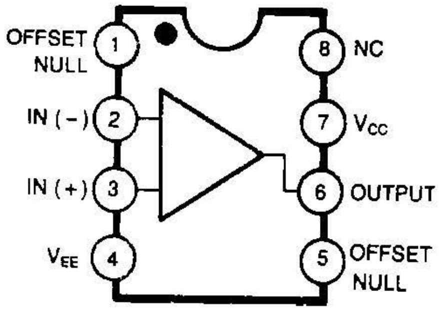

Rev. 1.0.1

©2001 Fairchild Semiconductor Corporation

APPENDIX B

Code of Humidity and Temperature Sensor (SHT11)

```
#include "cactus_io_SHT15.h"

int SHT_DataPin  = SDA;  // pin used for data
int SHT_ClockPin = SCL;  // pin used for clock
int voltage=A0;
SHT15 sht = SHT15(SHT_DataPin, SHT_ClockPin);
void setup()
{
  pinMode(A0,INPUT);
  Serial.begin(115200);
  Serial.println("Sensirion SHT15 Humidity - Temperature Sensor | cactus.io | Voltage");
  Serial.println("RH\t\tTemp (C)\tTemp (F)\tDew Point (C)\tVoltage");
}
void loop(){

  sht.readSensor();
  int voltageval = analogRead(voltage);

  Serial.print(sht.getHumidity()); Serial.print(" %\t\t");
  Serial.print(sht.getTemperature_C()); Serial.print(" *C\t");
  Serial.print(sht.getTemperature_F()); Serial.print(" *F\t");
  Serial.print(sht.getDewPoint()); Serial.print(" *C\t\t");
  Serial.print(voltageval,DEC);Serial.println(" V\t");
  // Add a 2 second
  delay(1000);

}
```

Figure B.1: SHT11 codes

Table B.1: Humidity, temperature, and capacitive sensor data

No.	Humidity (%)	Temperature (℃)	Voltage (mV)
1	0.43	33.66	460
2	0.43	33.55	460
3	0.44	33.28	468
4	0.45	32.95	468
5	0.46	32.60	468
6	0.46	32.23	468
7	0.47	31.91	472
8	0.48	31.60	472
9	0.49	31.30	472
10	0.50	31.02	472
11	0.50	30.78	472
12	0.51	30.55	472
13	0.51	30.32	472
14	0.52	30.12	472
15	0.52	29.90	472
16	0.53	29.71	472
17	0.53	29.57	472
18	0.54	29.40	472
19	0.54	29.27	472
20	0.54	29.14	472
21	0.55	29.06	472

22	0.55	28.94	472
23	0.55	28.81	472
24	0.56	28.73	472
25	0.56	28.61	472
26	0.56	28.50	472
27	0.56	28.42	472
28	0.57	28.32	472
29	0.57	28.24	472
30	0.57	28.16	472
31	0.57	28.08	472
32	0.57	28.01	472
33	0.58	27.96	476
34	0.58	27.88	472
35	0.58	27.82	472
36	0.58	27.76	476
37	0.58	27.70	476
38	0.59	27.66	476
39	0.59	27.61	476
40	0.59	27.56	476
41	0.59	27.52	476
42	0.59	27.48	476
43	0.59	27.46	476
44	0.59	27.43	476
45	0.59	27.41	476
46	0.60	27.37	478
47	0.60	27.34	478
48	0.60	27.32	478
49	0.60	27.32	478
50	0.60	27.30	478
51	0.60	27.26	480
52	0.60	27.26	480
53	0.60	27.25	480
54	0.60	27.24	480
55	0.60	27.20	480
56	0.60	27.20	480
57	0.60	27.18	480
58	0.60	27.18	482
59	0.60	27.16	482
60	0.60	27.16	482
61	0.60	27.14	482
62	0.60	27.13	482
63	0.60	27.13	482
64	0.60	27.11	482
65	0.60	27.12	482
66	0.60	27.12	482
67	0.60	27.12	482
68	0.60	27.09	482
69	0.60	27.08	482
70	0.60	27.08	482
71	0.60	27.07	482
72	0.60	27.06	482
73	0.60	27.06	488
74	0.60	27.06	482
75	0.60	27.04	488

76	0.60	27.04	488
77	0.60	27.02	488
78	0.60	27.00	488
79	0.60	26.98	488
80	0.60	26.96	488
81	0.60	26.94	488
82	0.60	26.94	488
83	0.60	26.93	488
84	0.60	26.91	488
85	0.60	26.90	488
86	0.60	26.87	488
87	0.60	26.86	488
88	0.60	26.85	488
89	0.60	26.83	488
90	0.61	26.82	488
91	0.61	26.82	488
92	0.61	26.77	488
93	0.61	26.76	490
94	0.61	26.73	488
95	0.61	26.74	488
96	0.61	26.71	490
97	0.61	26.71	490
98	0.61	26.70	488
99	0.61	26.69	488
100	0.61	26.68	488
101	0.61	26.66	492
102	0.61	26.67	492
103	0.61	26.68	492
104	0.61	26.69	492
105	0.61	26.70	492
106	0.61	26.70	492
107	0.61	26.70	488
108	0.61	26.74	488
109	0.61	26.72	488
110	0.61	26.72	488
111	0.61	26.72	488
112	0.61	26.74	488
113	0.61	26.74	488
114	0.61	26.73	488
115	0.61	26.73	488
116	0.61	26.73	488
117	0.61	26.75	488
118	0.61	26.75	488
119	0.61	26.74	488
120	0.61	26.72	488
121	0.61	26.74	488
122	0.61	26.76	488
123	0.61	26.75	488
124	0.61	26.76	488
125	0.61	26.75	488
126	0.61	26.75	488
127	0.61	26.75	488
128	0.61	26.76	488

APPENDIX C

The Capacitance value measure with LCR meter

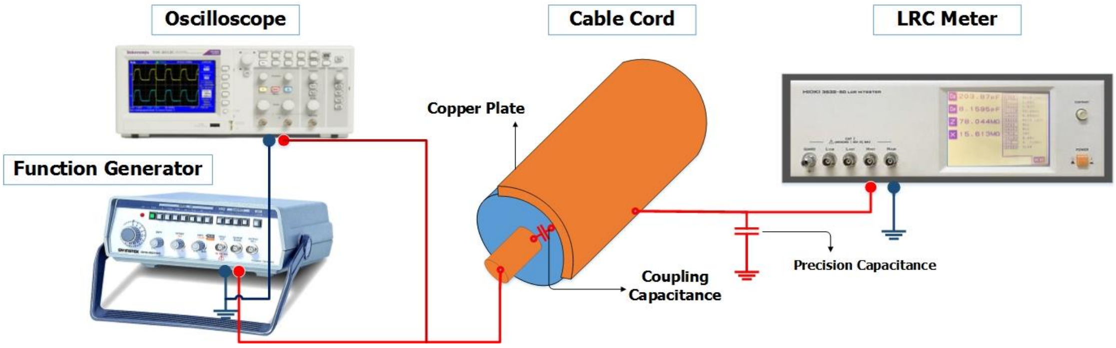

Figure C.1: The prototype of the capacitive sensor connected to LRC

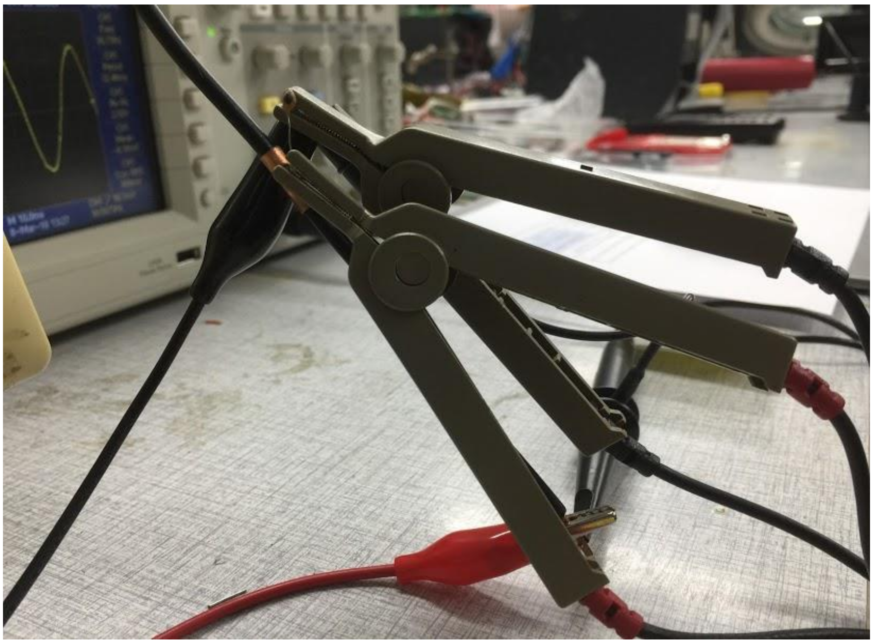

Figure C.2: the capacitive sensor and precision capacitor were clipped

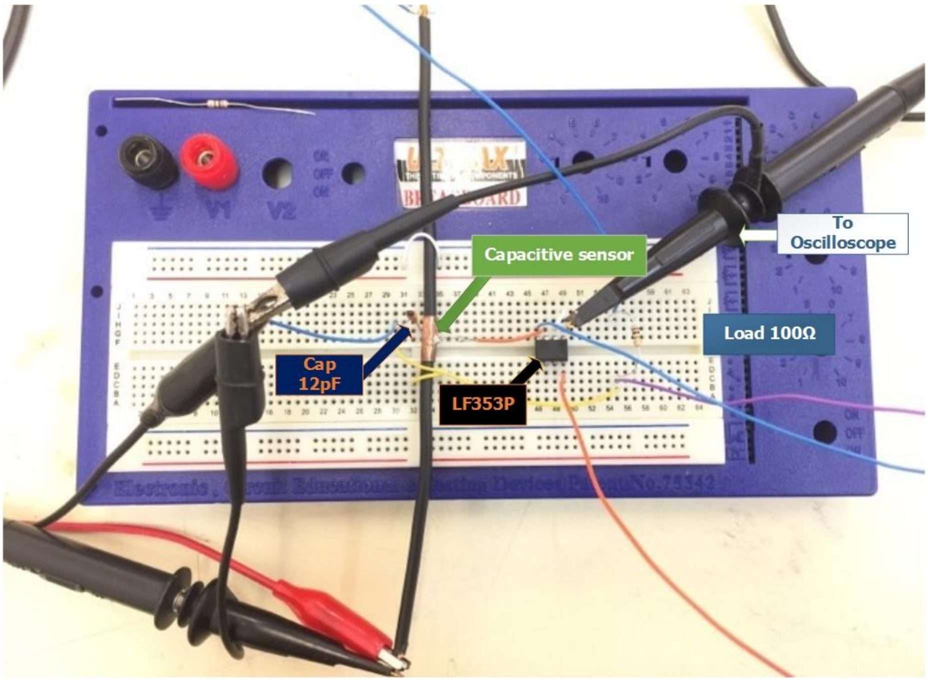

Figure C.3: The capacitive sensors connected to the LF353P

APPENDIX D

Image of the newly proposed circuit and analog front-end

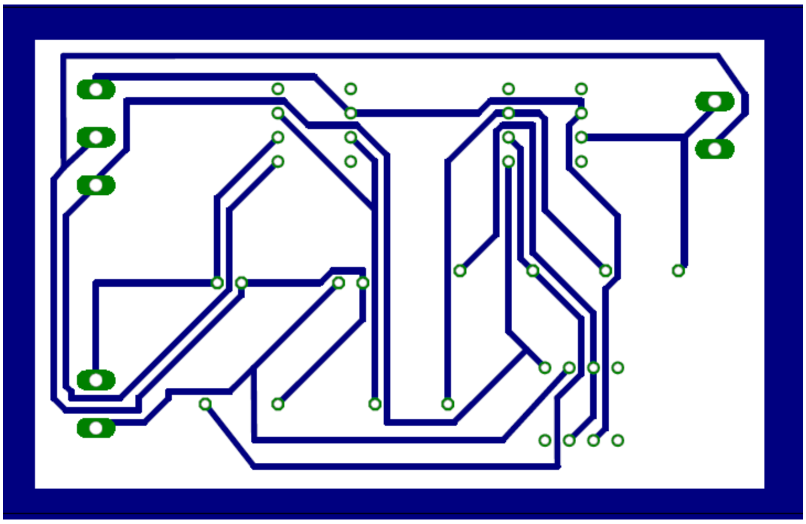

Figure D.1: PCB board designed for analog front-end

Figure D.2: The capacitive sensors wrapped on cables

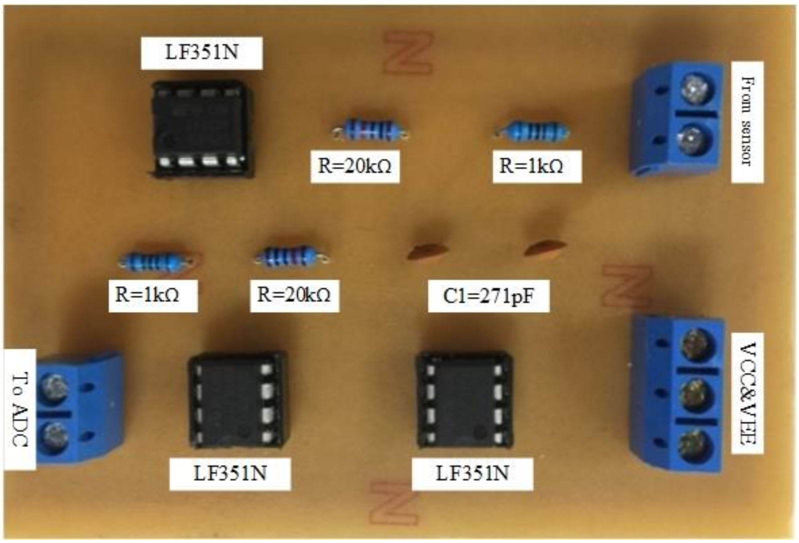

Figure D.3: The analog front-end board

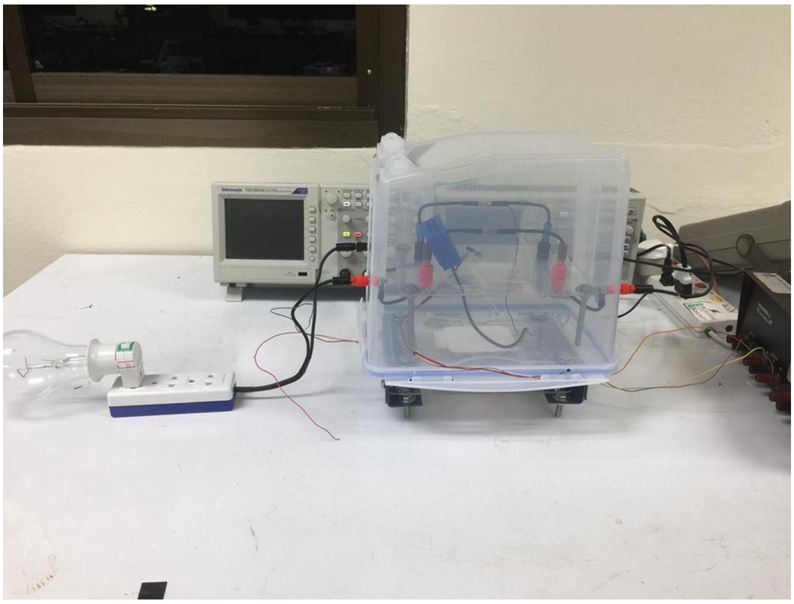

Figure D.4: The proposed system

VITAE

Name Sotara REN

Student ID 5910120082

Educational Attainment

Degree	Name of Institution	Year of Graduation
Master of Engineering (Electrical Engineering)	Prince of Songkla University	2018
Master of Information Technology	University of Puthisastra (Cambodia)	2016
Bachelor of Computer Science (Programming and Database)	University of Puthisastra (Cambodia)	2014
Technician Degree (Electrical and Electronic Engineering)	Institute of Technology of Cambodia (Cambodia)	2013

Scholarship Awards during Enrolment

The Royal Scholarships under Her Royal Highness Princess Maha Chakri Sirindhorn Education Project to the Kingdom of Cambodia for Master Degree Program.

List of Publication

R. Sotara, H. Nakahara, K. Thongpull, P. Phukpattaranont, and K. Chetpattananondh, "A development of capacitive voltage sensor for non-intrusive energy meter," *2018 15th International Conference on Electrical Engineering/Electronics, Computer, Telecommunications and Information Technology (ECTI-CON)*, 18-21 July 2018, pp. 270–273.